Glacier inventories reveal an acceleration of Heard Island glacier loss over recent decades

Levan G. Tielidze[1,2], Andrew N. Mackintosh[1,3], Weilin Yang[3]

[1]Securing Antarctica's Environmental Future, School of Earth, Atmosphere and Environment, Monash University, Clayton, VIC 3800, Australia

[2]School of Natural Sciences and Medicine, Ilia State University, Tbilisi 0162, Georgia

[3]School of Earth, Atmosphere and Environment, Faculty of Science, Monash University, Clayton, VIC 3800, Australia

Abstract

Glacier inventories provide baseline data for understanding and evaluating past, current, and future changes in glacier extent in response to climate changes. We present a multi-year, manually mapped glacier inventory for sub-Antarctic Heard Island, a remote glacier-covered volcano in the southern Indian Ocean. Glacier outlines are presented for 1947, 1988, and 2019, derived from large-scale topographical maps (1:50,000), cloud-free medium-resolution SPOT, and high-resolution Pléiades satellite orthoimages. ASTER and Pléiades digital surface elevation models for 2000 and 2019 were also used to determine topographic parameters for individual glaciers. Heard Island glacier area reduced from 289.4±6.1 km^2 in 1947 to 260.3±6.3 km^2 in 1988, further decreasing to 225.7±4.2 km^2 in 2019. The rate of annual glacier area loss between the two observation periods (1947-1988 and 1988-2019) almost doubled from −0.25% yr^{-1} to −0.43% yr^{-1}. Glaciers on the eastern slopes of Heard Island experienced much higher retreat rates than glaciers elsewhere on the island. The maximum retreat observed between 1947 and 2019 was ~5.8 km for the east-facing Stephenson Glacier, where collapse of the terminus led to the formation of a large lagoon during recent decades. Surface debris cover on Heard Island glaciers increased from 7.0±6% (18.1 km^2) in 1988 to 12.8±5.5% (29.0 km^2) in 2019. We also observed an upward shift (4.2 m yr^{-1}) in the maximum elevation of debris cover from 285±20 m a.s.l. (above sea level) to 605±20 m a.s.l., during this time. Direct climate observations from Heard Island are scarce, but climate reanalysis ~~climate~~ data show that the decline in glaciers is associated with a rising temperature of 0.7°C over the last seven decades. ~~Many questions about the behaviour of Heard Island glaciers remain unanswered.~~ Our inventory dataset will be freely available in the GLIMS glacier database to facilitate further analysis and modelling of Heard Island glaciers.

Correspondence: Levan G. Tielidze (tielidzelevan@gmail.com)

Keywords: Heard Island, glacier inventory, remote sensing, debris cover, glacier retreat.

1 Introduction

Glaciers are a key component of the climate system and serve as sensitive indicators of climate change (Hock et al., 2019). Over recent decades, global glaciers—excluding the Greenland and Antarctic ice sheets—have contributed approximately 27 ± 22 mm to the rise in global mean sea level from 1961 to 2016 (Zemp et al., 2019), including approximately 5.5 mm between 2006 and 2015 (IPCC, 2019). This represents 25 to 30 percent of the total sea level rise during that period (Zemp et al., 2019). Glacier shrinkageretreat also has a fundamental impact on global water supplies and mountain hazards (Hock et al., 2019) and glacier inventories are essential for assessing all these impacts (Haeberli and Hoelzle 1995; Huss and Hock, 2018; Hugonnet et al., 2021; Rounce et al., 2023;). Inventories include digitized glacier outlines and their morphological features, such as area, slope, aspect, and elevation, mapped from satellite images and Digital Elevation Models (DEMs). In combination with glacier outlines theyThey provide crucial data for estimating geodetic mass balance (Shean et al., 2020), determining glacier volume (Farinotti et al., 2019), measuring surface velocity (Dehecq et al., 2019), and testing glacier models (Radić et al., 2014; Eis et al., 2021).

Given the scarcity of landmasses and climate observations in the Southern Ocean region, glacier-covered sub-Antarctic islands provide a unique window into the impacts of past, present, and future climate changes (e.g. Deline et al., 2024). Heard Island is such an example but because of its harsh climate and remote location and harsh climate, its glaciers remain relatively poorly studied compared to other mid-latitude glaciers in the Southern Hemisphere. A new inventory from this region offers critical data on glacier behaviour, such as area and terminus changes, which are essential for understanding how these glaciers are responding to climate changes and other drivers. Given the limited field-based research opportunities on Heard Island, a new glacier inventory also allows us to analyse past glacier conditions, improving our understanding of processes and providing a baseline for predicting future changes in this sensitive region.

Heard Island is an UNESCO World Heritage site due to its outstanding physical and biological features which are being affected by significant on-going climatic changes. As one of the only sub-Antarctic islands mostly free of introduced species, its largely undisturbed ecosystems are particularly at risk from the impact of human settlementsglacier retreat (HIMI Management Plan, 2014). This is because ice recession causes long-isolated ecological communities to become connected, likely favouring generalist species which will increase ecological connectivity glacier retreat (HIMI Management Plan, 2014(Bosson et al., 2023). Glacier inventory work will help in designing effective conservation strategies and managing protected areas to ensure the preservation of the biodiversity they support (Pockley, 2001; HIMI Management Plan, 2014).

Since a complete inventory of Heard Island glaciers has not been published for several decades (e.g. Budd, 2000; Allison and Thost, 2000; Thost and Truffer, 2008), this study

aims to create a new inventory using remotely sensed glacier parameters. We use our analysis to assess how various climatic, morphological and topographic factors influence glacier recession on Heard Island, providing preliminary answers to the question of how ~~and why~~ Heard Island glaciers are changing.

2 Study area

2.1 Physical characteristics

Heard Island is the largest member of the Territory of Heard Island and McDonald Islands located at 53°05'S latitude and 73°31'E longitude at the southern edge of Indian Ocean, almost midway between western Australia and South Africa. Antarctica is the nearest continent, located ~1500 km to the south, while the relatively large Kerguelen Islands are ~450 kilometers to the northwest. Heard Island is approximately 40 km long from northwest to southeast, and only 20 kilometers wide from northeast to southwest (Figure 1).
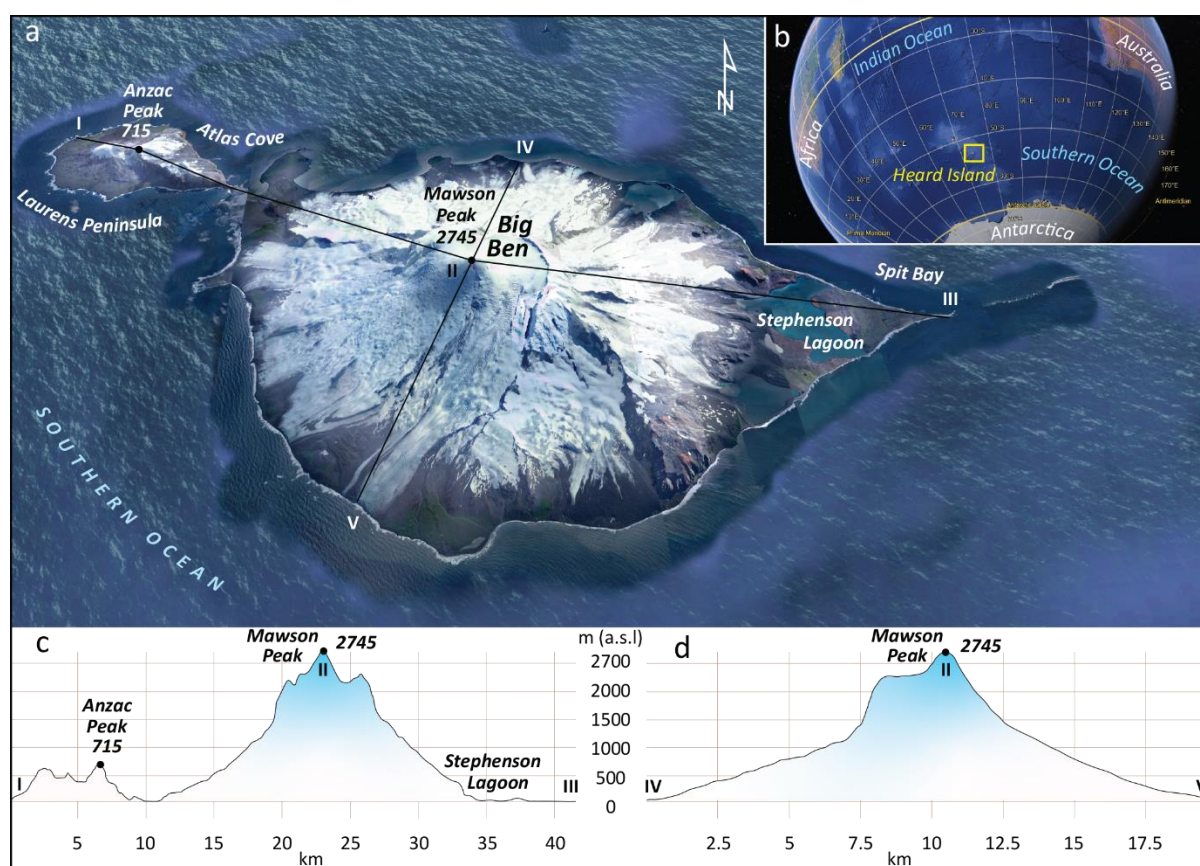
Figure 1. True colour aerial image of the Heard Island (© Google Earth). b - location of the Heard Island in the Southern Hemisphere (© Google Earth). c - Longitudinal and d - transverse profiles (cross sections) of Heard Island.

Heard Island, along with the McDonald Islands and Kerguelen Island, forms part of the submarine Kerguelen Plateau, a significant geological feature in the southern Indian Ocean. Heard Island's geological structure is characterized by its two volcanic cones — Big Ben and Laurens Peninsula — each with distinct elevations and volcanic rocks and landforms. Big Ben, with a diameter of ~20 km and reaching an elevation of 2,745 m asl at Mawson Peak, is the larger volcanic cone. The highest point of the Laurens Peninsula is Anzac Peak (715 m asl). Over 80% of the Heard Island is ice-covered with glaciers (Thost and Truffer, 2008) flowing from the caldera of Big Ben and the summit plateau of Laurens Peninsula. Big Ben was most recently reported active in November 2020 (Fox et al., 2021).

The climate of the Heard and McDonald Islands region is significantly shaped by its mid-latitude position in the Southern Ocean, south of the Antarctic Polar Front, where subantarctic and colder Antarctic Ocean waters converge. This location is affected by the region's westerly winds, which are linked to the west-to-east progression of deep low-pressure systems in the mid to high southern latitudes (Allison and Keage, 1986). Heard Island's weather is characterized by small variations in both seasonal and daily temperatures, with persistent cloud cover, frequent precipitation, and strong winds. Snowfall occurs year-round. Based on various observations from the second half of the 20th century (Kiernan and McConnell, 2002; HIMI official website, last access: August 2024), average monthly temperatures at Atlas Cove range from 0.0 to 4.2°C. In summer, daily temperatures typically vary between 3.7 and 5.2°C, while in winter, they range from −0.8 to 0.3°C. The winds are predominantly westerly and strong, with monthly average speeds at Atlas Cove varying between ~26 and 33.5 km/h. Gusts can exceed 180 km/h. Heard Island experiences annual precipitation at sea level ranging from 1,300 to 1,900 mm, with rain or snow occurring on roughly three out of every four days. However, meteorological records for the island are scarce and incomplete and long-term local observations including information about local gradients and trends are absent.

2.2 Previous studies

Heard Island became widely known after 1853 when Captain Heard visited the site, although it was first seen by Captain Peter Kemp in 1833 (Mawson, 1935). Two years after Captain Heard's expedition, Darwin Rogers was the first to land on Heard Island in 1855 (Lambeth, 1951). Following this, sealers occupied the island from the mid to late 19th Century, decimating the seal population. Later, various scientific expeditions visited Heard Island and stayed only several days, mainly at Atlas Cove (e.g. Drygalski, 1908; Aubert de la Rue, 1929; Mawson, 1932).

The largest scientific campaign began in 1947, when the Australian National Antarctic Research Expedition established a base camp at Atlas Cove. This campaign continued until 1955, and James Lambeth first carried out physical measurements of Heard Island glaciers at this time (Lambeth, 1951). According to his notes the snow line of the Heard

Island glaciers was at about 305 m a.s.l. in Austral summer of 1947-1948. There was minor difference in the snowline elevations between north- and south-facing glaciers. Thickness of the Baudissin and Vahsel glaciers at the frontal area was between 35-40 m in August 1948. Ice velocity measurement at an elevation of 90 m a.s.l. of Baudissin Glacier tongue between 11 September and 8 December indicated an average ice flow rate of approximately 440 m a^{-1}, while the ablation at an elevation of about 40 m a.s.l. was ~−0.35 m during this ~33-month period. A rRecent global study of glacier thickness and velocity (Millan et al., 2022) based on Landsat and Sentinel image pairs acquired between 2017 and 2018, shows unusually fast flow velocities for the Gotley Glacier with velocities up to 1,500 m a^{-1}.

Short scientific visits to the island were also made in 1963, 1965 and 1969 mainly for seasonal observation of the north-facing glacier front variations (Budd, 1964; 1970; Budd and Stephenson, 1970). More detailed studies of Vahsel Glacier, including mass balance measurements started later in 1971 (Allison, 1980). Ablation at 200 m a.s.l. was estimated at 3-4 metres water equivalent annually. A surface velocity profile across the glacier at the same elevation showed annual movement of 200-280 m near the centre. Average thickness of Vahsel Glacier (determined gravimetrically) below the equilibrium line, was between 60-80 m near the centreline.

Studies of south and southeast facing glaciers starter later in 1990s. The retreat and proglacial lake expansion at Stephenson Glacier was studied by Kiernan and McConnell (2002), who showed that the glacier retreated at a mean rate of -18 ma^{-1} from 1947 to 1987 before accelerating dramatically to -100 m a^{-1} between 1987 and 2000. Further glaciological and meteorological study of Brown Glacier on the eastern slope of Heard Island was conducted by Thost and Truffer (2008) based on old topographical maps (1947) and ground-based observations (2004). They concluded that Brown Glacier area decreased by ~29% during the investigated period, while on average the surface lowered by −0.50 m a^{-1}. This mass loss was consistent with interpolated summer (January-March) temperatures in the area that indicated a +0.9 °C warming over the investigated period (1947-2004). They also observed that the Brown Glacier terminus retreated by 63 m between 2000 and 2003.

The GLIMS book (Kargel et al., 2014) identifies 29 glaciers on Heard Island with a total area of 257 km^2 in 1988 (Cogley et al., 2014), while the Randolph Glacier Inventory (RGI6) database identifies 31 glaciers with a total area of 254.4 km^2 (Pfeffer et al., 2014). Some glaciers in these datasets have incorrect terminus positions, specifically the eastern-facing glaciers, and nearly all glaciers are also characterized with inaccurate ice margins (due to misidentification of ice divides). This issue persists in the RGI7 database (Maussion et al., 2023).

3 Data sources

Conducting large-scale field-based glacier research on Heard Island is extremely challenging due to topographic, logistical, financial, and safety obstacles (e.g. Allison and Thost, 2000). Consequently, old topographical maps and remotely sensed images from historical and current Earth observation platforms provide the most viable method for tracking changes in glacier parameters (e.g. Tielidze, 2016; Freudiger et al., 2018; Weber et al., 2020).

3.1 Old maps

The first aerial photographs of Heard Island glaciers were captured in 1947 using a hand-held 6" x 6" Fairchild F24 camera aboard an RAAF Walrus amphibious aircraft. These photos provided limited oblique coverage of the east and north coasts. However, a ground triangulation survey conducted in 1948, which focused on Laurens Peninsula and the north and east coasts, allowed for more accurate mapping of terrain features, including glacier fronts (Allison 1980). A large scale (1:50,000) topographical map of Heard Island (1964) shows glacier boundaries from 1947-1948 based on these early photographs and surveys (Division of National Mapping, 1964). Therefore, the glacier extent on Heard Island in 1947-1948 can be directly referenced from this topographical map, which reflects the original positions of the glaciers as depicted in the aerial images (Figure 2; Table 1).

197
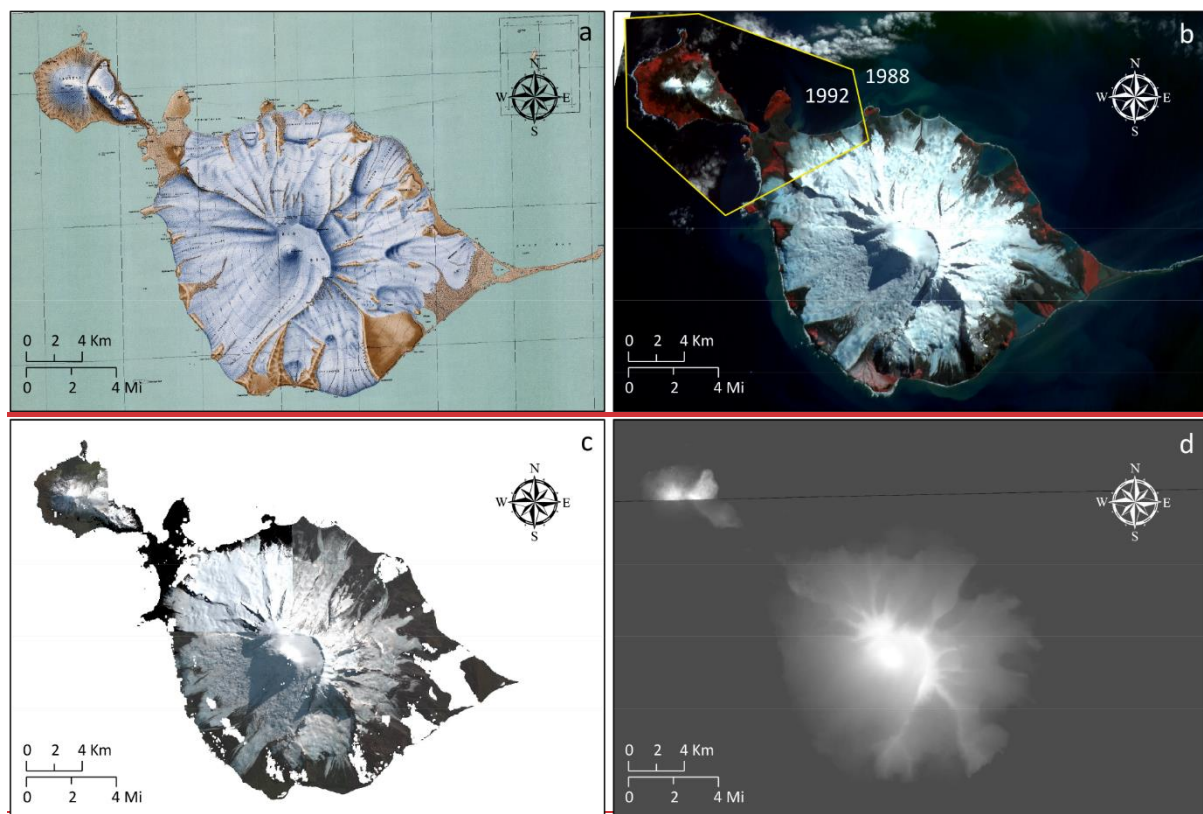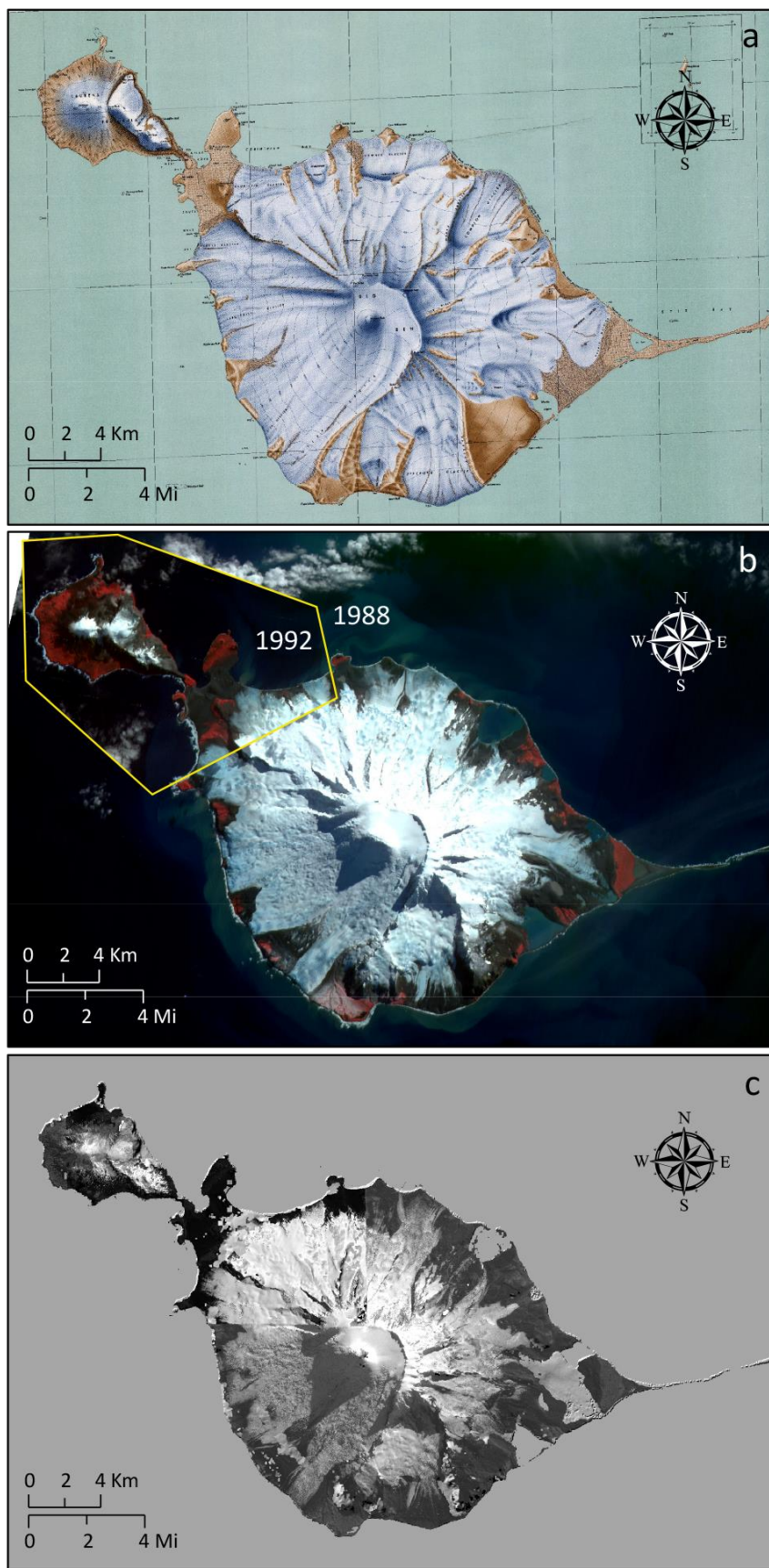
Figure 2. Data sources used in this study for glacier mapping. a – Topographical map from
1964 compiled based on aerial imagery from 1947. b – SPOT images from 1988 and 1992.
c – Pléiades images from 2019, d – ASTER DEM from 2000.

3.2 Satellite images

Landsat satellite products have been available since the 1980s, although image acquisition was limited in early 1990s due to its commercial phase (Williamson, 1997). Post-1990s Landsat images of Heard Island often feature cloud cover that partially or completely obscures glaciers, making it difficult to accurately delineate glacier boundaries. ~~Although Landsat satellite products have been available since the 1980s, the frequent cloud cover around Heard Island has obscured the glaciers partially or completely, making it difficult to accurately delineate glacier boundaries.~~ We therefore use medium-resolution (10 and 20 m) cloud-free SPOT 1 images from 1988 and 1992 available from the French Space Agency (CNES)'s Spot World Heritage Programme (https://regards.cnes.fr/html/swh/Home-swh3.html, accessed August 2024). The 1988 image was used as the baseline database, and the 1992 image was used as a supplement because the Laurens Peninsula and northern parts of the Heard Island glaciers were partly covered by clouds in 1988 image.

A 2-metre resolution, georeferenced, cloud-free Pléiades ortho mosaic and 0.5-metre resolution panchromatic bands from 2019 austral summer were used to delineate the most recent glacier boundaries in our data set. These images were not available for the northwest part of the Laurens Peninsula. To fill this gap, we used similar Pléiades product acquired in April 2018, but the images from 2019 were used as a main dataset for the island. Pléiades images were received from the Laboratory of Space Geophysical and Oceanographic Studies (LEGOS) via the Pléiades Glacier Observatory (Berthier et al., 2024).

High-resolution QuickBird images (2014-2024), combined with SRTM3 topography data (Raup et al., 2014), were also used in Google Earth Pro software to enhance the 3D visualization and identification of ice divides as well as to validate the glacier outlines mapped from the satellite images.

For the annual measurements of Stephenson and Brown glacier termini, a 30 m resolution Landsat 7 Enhanced Thematic Mapper Plus (ETM+) and 10 m resolution Sentinel 2 images were used, as they only had cloud-free windows for these two glaciers. Both Landsat and Sentinel products are from the Earth observation (EO) Browser (https://apps.sentinel-hub.com/eo-browser/ accessed August 2024).

3.3 Digital elevation/surface models

Topographic parameters of glaciers such as aspect, slope, and elevation from 1947 and 1988 were obtained from the Advanced Spaceborne Thermal Emission and Reflection Radiometer Global Digital Elevation Model (ASTER GDEM ~~V2~~V3, March 1, 2000), available through the EarthExplorer (http://earthexplorer.usgs.gov/, accessed May 2024), U.S.

Geological Survey (USGS), with a horizontal resolution of 20 meters (Tachikawa et al., 2011). The ASTER GDEM is widely recognized and used in glaciological research globally across different spatial scales (e.g. Bhambri et al. 2011; Stokes et al., 2013; Tielidze et al., 2020). The same topographic characteristics for the glaciers from 2019 were extracted from the high-resolution (2 m) Pléiades Digital Surface Models (DSM) 2018-2019 available from the Laboratory of Space Geophysical and Oceanographic Studies (LEGOS) via the Pléiades Glacier Observatory (Berthier et al., 2024).

Table 1. Topographic maps, satellite images and digital elevation/surface models used in this study.

Product	ID	Date	Resolution/Scale
Map			
Topographical map	G9182.H4	1964 (1947)	1:50 000
Satellite image			
SPOT 1	1 245-457 88-01-09 04:47:36 1 X	09/01/1988	10 m
SPOT 1	2 245-458 92-03-24 05:00:31 1 X	24/03/1992	20 m
Landsat 7 ETM+	LE07_L2SR_135097_20010131_20200917_02_T1	31/01/2001	30 m
Landsat 7 ETM+	LE07_L2SR_135097_20030105_20200916_02_T1	05/01/2003	30 m
Landsat 7 ETM+	LE07_L2SR_135097_20040312_20200915_02_T2	12/03/2004	30 m
Landsat 7 ETM+	LE07_L2SR_135097_20050126_20200914_02_T1	26/01/2005	30 m
Landsat 7 ETM+	LE07_L2SR_135097_20080204_20200913_02_T1	04/02/2008	30 m
Landsat 7 ETM+	LE07_L2SR_135097_20090206_20200912_02_T1	06/02/2009	30 m
Landsat 7 ETM+	LE07_L2SR_135097_20100209_20200911_02_T1	09/02/2010	30 m
Sentinel 2 L2A	42/F/YF/2017/4/16/0/	16/04/2017	10 m
Pléiades	0444140_Heard_ANT_1B	22/04/2018	0.5-2 m
Pléiades	0451575_Heard_ANT_1B	07/04/2019	0.5-2 m
Pléiades	0452069_Heard_ANT_1B	07/04/2019	0.5-2 m
Pléiades	0448386_Heard_ANT_1A	21/11/2019	0.5-2 m
Digital elevation/surface model			
ASTER	ASTGTMV003_S53E073	01/03/2000	20 m
ASTER	ASTGTMV003_S54E073	01/03/2000	20 m
Pléiades	0444140_Heard_ANT_1B	22/04/2018	2 m
Pléiades	0451575_Heard_ANT_1B	07/04/2019	2 m
Pléiades	0452069_Heard_ANT_1B	07/04/2019	2 m
Pléiades	0448386_Heard_ANT_1A	21/11/2019	2 m

4 Methods

4.1 Glacier mapping

Despite some advantages of the automated mapping method of clean ice (e.g. Paul et al., 2013), manual mapping of glaciers is more ~~suitable~~ accurate for many mountain regions around the world (e.g. Stokes et al., 2013; Nagai et al., 2016; Tielidze and Wheate,

2018; Korneva et al., 2024). In this study, glacier boundaries were, therefore, delineated manually. This was also mainly due to the i) unavailability of cloud-free satellite channels/bands for different years for the entire study area, which limited us to use different band ratio segmentation methods for automated mapping; ii) significant amount of debris-cover, which can cause uncertainty during automatic mapping or hinder mapping; and iii) a relatively small study area, which was less time expensive than it would have been for an entire mountain range.

4.2 Terminus measurement

Accurately quantifying changes in glacier termini is essential for effective monitoring of glacier changes over various timescales, from days years to centuries. Methods for this technique each offer advantages and limitations (Lea et al., 2014). In this study, we only measured two glacier (Stephenson and Brown) lengths based on the Global Land Ice Measurements from Space (GLIMS) guidelines (www.glims.com) and by following Purdie et al. (2014). The flow direction of the glacier was manually determined to be perpendicular to altitude contours. We assessed terminus changes by comparing glacier outlines from different dates along the ice front, oriented perpendicular to the flow. Elevation changes at the glacier fronts were also measured at the intersection points.

4.3 Accuracy and uncertainly assessment

When using glacier outlines to assess changes, it's crucial to understand their accuracy. Assessing accuracy can be difficult because high-resolution reference data are often scarce. Additionally, any manual corrections made to the raw outlines (e.g. such as debris cover) may reflect the bias of the analyst rather than the effectiveness of the algorithm used (Paul et al., 2013). It is therefore essential to establish an uncertainty even after achieving high-accuracy mapping. Uncertainty often arises from the resolution of the satellite image, and from the contrast between the glacier and the surrounding terrain (Burgess and Sharp, 2004; DeBeer and Sharp, 2007).

To estimate glacier mapping uncertainty, first we tested multiple digitization (e.g. Paul et al., 2013; Tielidze et al., 2022). A sub-sample of two glaciers from the medium-resolution SPOT image, 1988, were re-digitized by three different operators. The selected glaciers included debris-free Brown and one unnamed debris-covered, glacier with Glims ID of G073625E53121S. The uncertainty for the debris-free Brown Glacier based on normalized standard deviation (NSD – delineations by multiple digitalization divided by the mean glacier area for all outlines) was 2.0 %. In contrast, the debris-covered glacier exhibited a much higher uncertainty of 5.3%. We applied the same methodology to these glaciers using the high-resolution Pléiades image from 2019. The mapping uncertainty for the debris-free glacier was determined to be 1.1%, while the debris-covered glacier exhibited a considerably higher uncertainty of 5.1% (Figure 3a-d).

294 -To estimate the statistical uncertainty for each glacier, we used the buffer method as in
295 Granshaw and Fountain (2006) and Bolch et al. (2010). This approach provides a
296 minimum and maximum area values, which we utilized to calculate the relative area
297 difference. For the 1:50,000 scale topographic map, or glacier outlines from 1947, a 30 m
298 buffer size proposed by Tielidze (2016) was used, yielding a total potential error of ±2.1%.
299 A 20 m buffer was used for 1988 glacier outlines giving a total error of ±2.4%. The chosen
300 buffer is based on a previous multiple digitizing experiment from similar resolution
301 satellite images worldwide (Paul et al., 2013; Tielidze and Wheate, 2018), demonstrating
302 that the variability in positioning typically falls within one pixel, or approximately ±10-30
303 meters, depending on the image resolution. Despite the high resolution of the Pléiades
304 images, we choose a 10 m buffer size for glacier contours from 2019 estimating a total
305 uncertainty of ±1.9%. This decision is primarily due to an extensive debris cover, which
306 frequently complicates the mapping of glaciers.

307 A larger buffer should be applied to the debris-covered parts of glaciers, as ~~outline~~outline
308 uncertainties are higher than for bare ice (e.g., Tielidze et al., 2020). In our case, the buffer
309 size was set to 30 meters, resulting in a total potential error of ±6.0% for 1988 and ±5.5%
310 for 2019 glaciers. We have not estimated the surface debris cover for the glaciers from
311 1947.

312 For uncertainties in length changes, we used the source image resolution as proposed by
313 Hall et al. (2003).

314
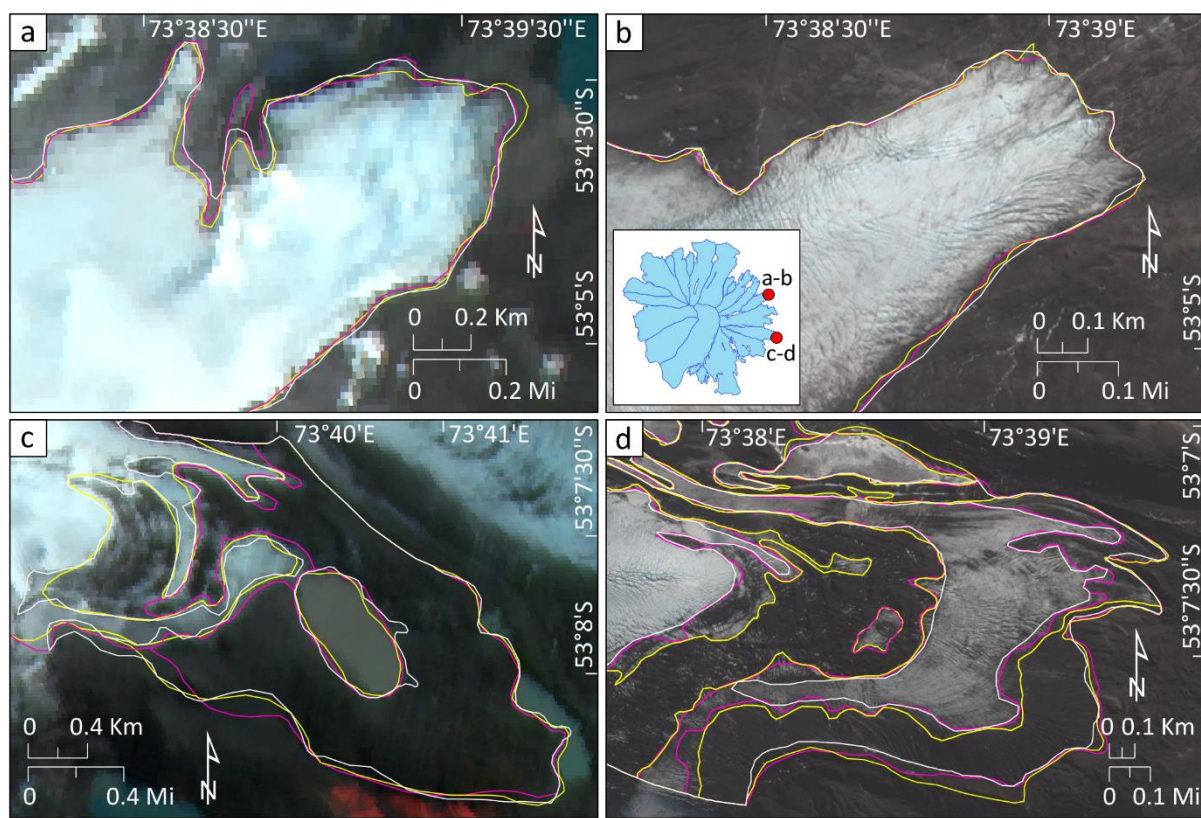
315 **Figure 3**. An example of multiple digitization for debris-free Brown (a-b) and debris-
316 covered G073625E53121S (b-c) glacier terminus. a-c - SPOT scene (09/01/1988). b-d -

5 Results

5.1 Glacier area changes in 1947-1988-2019

A total of 29 glaciers, with an average size of 9.9 km^2, were mapped in the study area in 1947 (Figure 34). During the 41-year observation period from 1947-1988, the glaciers shrank by 29.1±0.7 km^2 (10.1%) from 289.4±6.1 km^2 in 1947 to 260.3±6.3 km^2 in 1988, showing a mean annual glacier area loss of −0.25% yr^{-1}. 30 glaciers were identified in 1988 with an average size of 8.7 km^2. Between 1988 and 2019, a considerable decrease in glacier area of 34.6 km^2 (13.3%) to 225.7±4.2 km^2 occurred, almost doubling the rate of annual glacier area loss to −0.43% yr^{-1}. The average glacier size also decreased to 6.4 km^2 during this period.

335

336

337
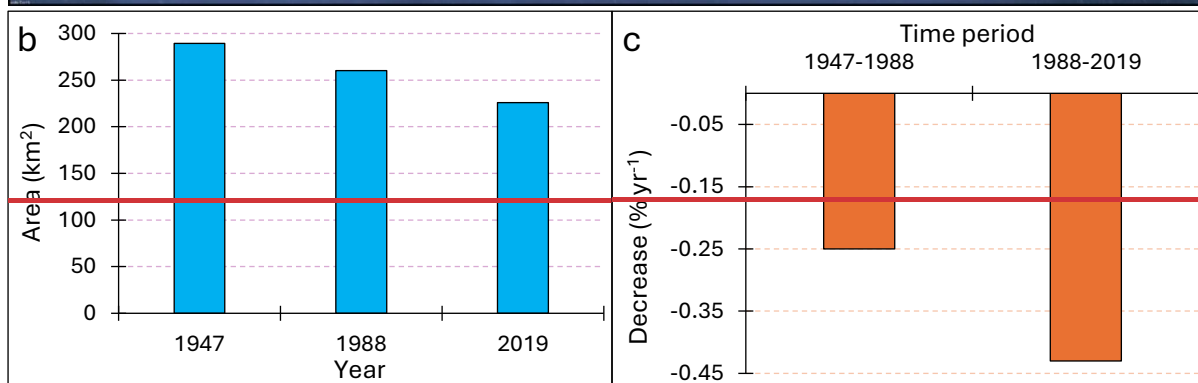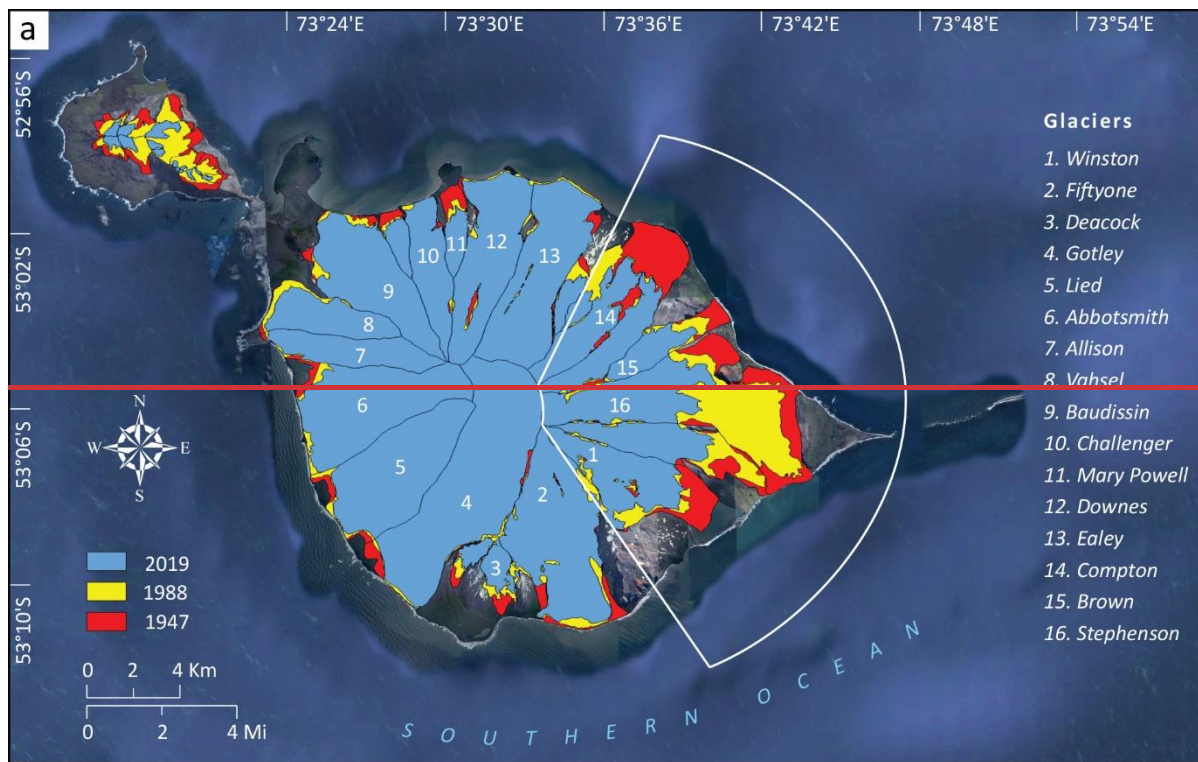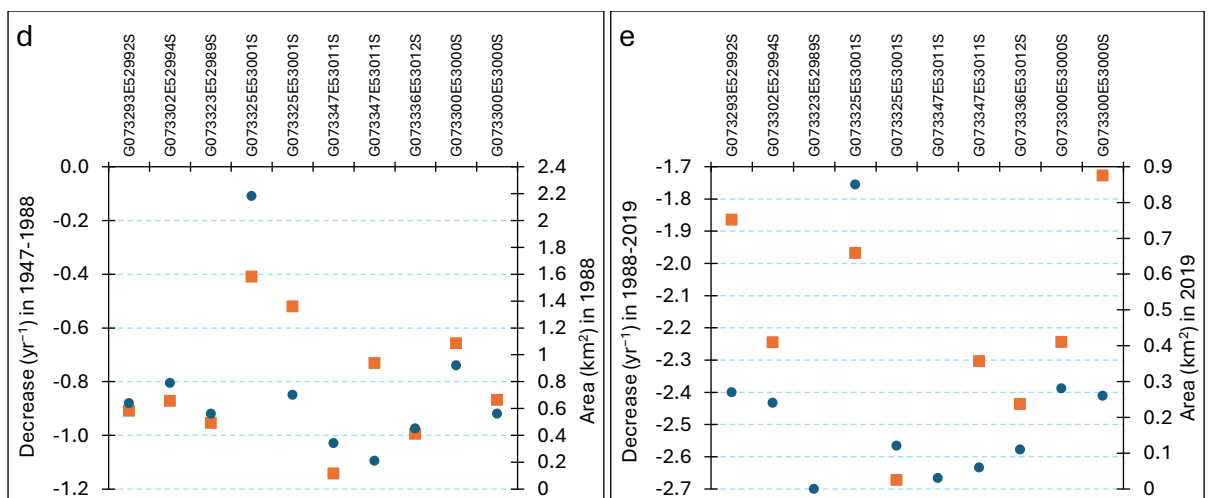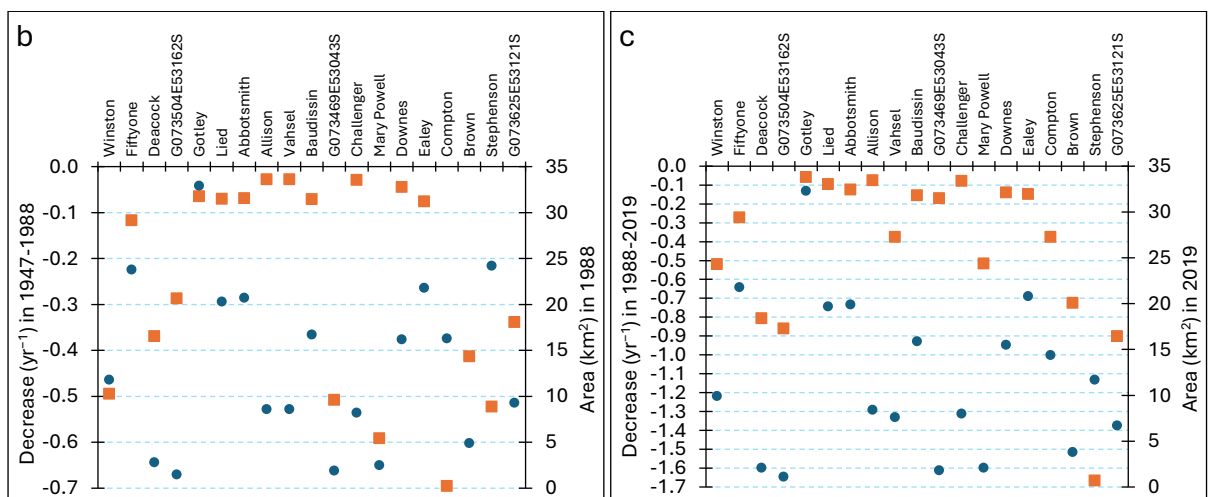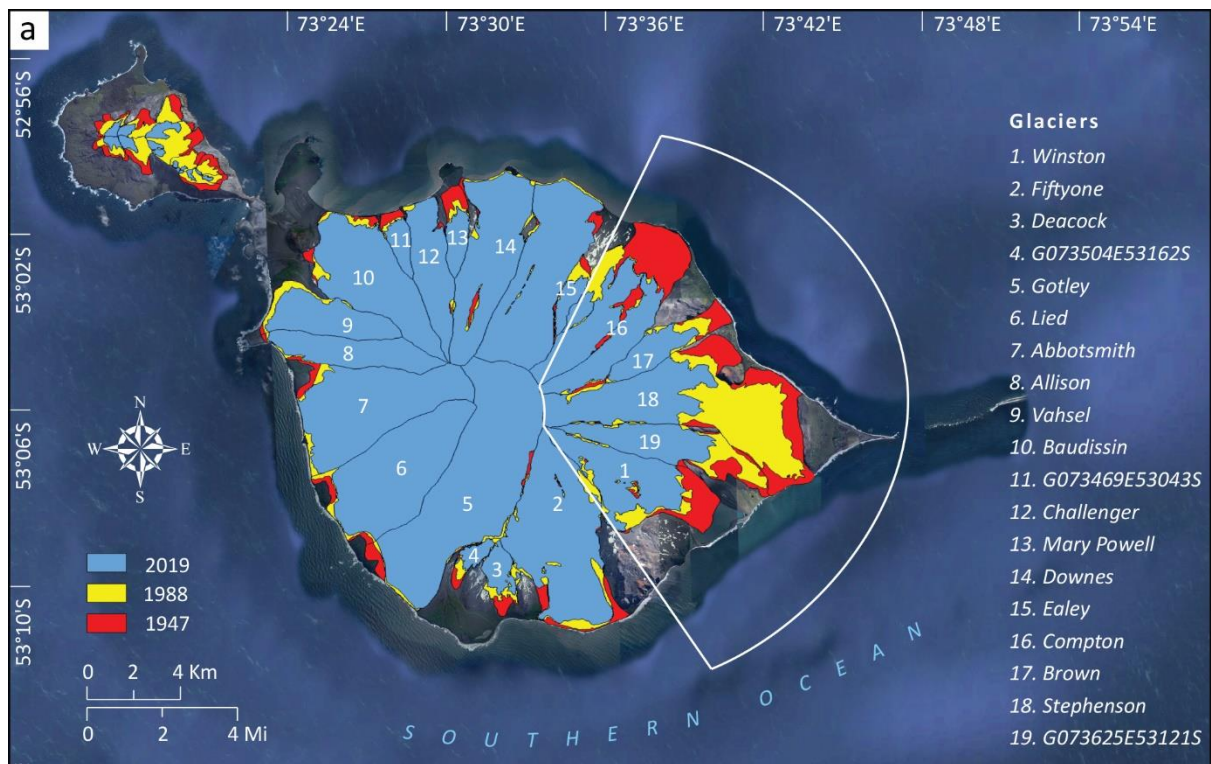
Figure 34. a - Heard Island glacier outlines in 1947, 1988, and 2019. The white frame highlights east-facing glaciers where the highest decrease rates occurred. ~~b - Heard Island glacier areas in 1947, 1988, and 2019; c - Glacier area decrease rates for the Heard Island for the two observed periods (1947-1988 and 1988-2019).~~ A scatter plot of the individual glacier annual area changes rate is also shown (brown dots) vs. glacier size (blue dots) for the Big Ben (b-c) and for the Laurens Peninsula (d-e).

The pattern of observed glacier wastage is strongly influenced by topographic and morphological parameters. The small and low elevation glaciers at Laurens Peninsula experienced largest change in area from 10.5 km² to 2.2 km² between 1947-2019. This is an area loss of −79±2.2% amounting to an annual decrease of −1.1% yr⁻¹ (Figure 4b-e).

We also observed upward shift of the minimum and mean elevation of all Heard Island glaciers during the study period and downward shift of the maximum elevation from 1988 (Figure 45). Lowering trend of the maximum elevation is mainly due to the small glacier disappearances from the Laurens peninsula.
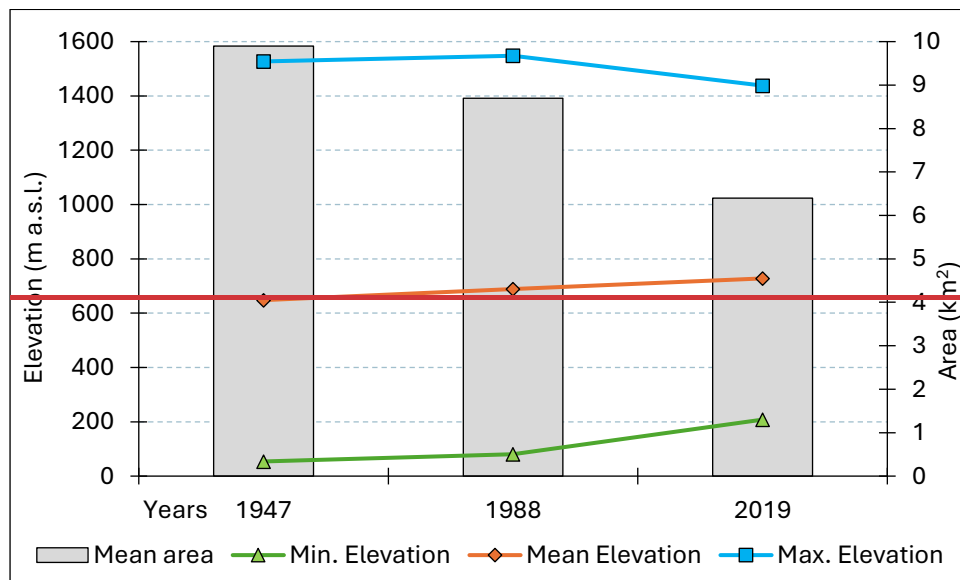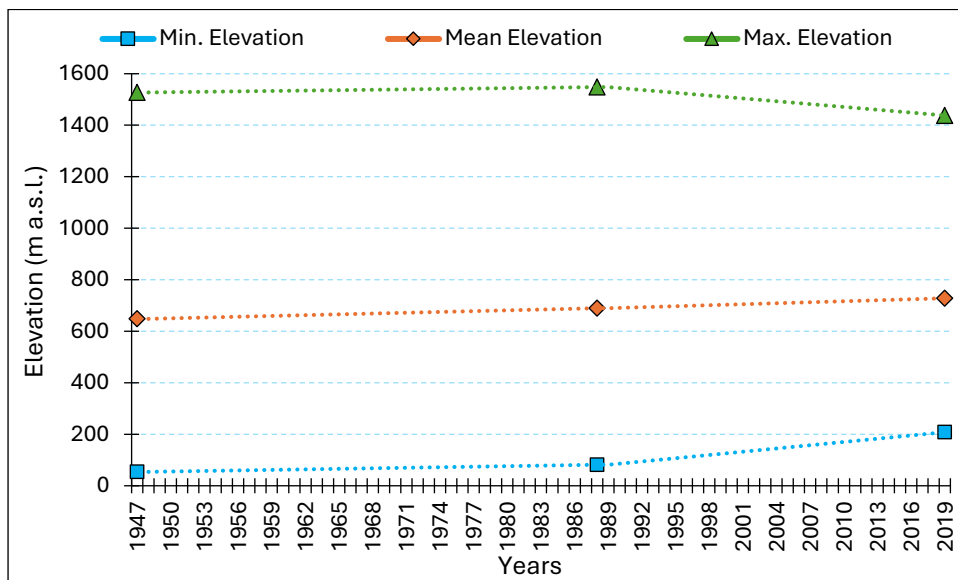
Figure ~~4~~5. Changes in Heard Island glacier ~~area and~~ minimum (Min.), mean, and maximum (Max.) elevations between 1947-1988-2019. ~~Mean area, minimum (Min.), mean, and maximum (Max.) elevations are shown.~~

Gotley Glacier was largest on Heard Island in 2019, with an area of 32.3 ± 0.5 km^2, followed by Fiftyone and Abbotsmith glaciers with areas of 21.8 ± 0.4 and 19.9 ± 0.3 km^2, respectively.

By number, most glaciers on Heard Island are oriented towards the northeast, whereas most of the area is facing southwest. ~~The inventory shows that Heard Island glaciers are predominantly oriented towards the northeast, while the largest glaciers are oriented southwest.~~ Glaciers of west and southwest orientation have the highest mean elevations (Figure ~~5a~~6a-c).

Eastern facing glaciers experienced the highest area loss over the study period (depicted by the white outline in Figure ~~3a~~4a) from 85.1 ± 1.6 km^2 in 1947 to 66.5 ± 1.3 km^2 in 1988 and 46.3 ± 0.9 km^2 in 2019. This was a 22% or −0.53% yr^{-1} decrease between 1947-1988 which is more than double than the change for all Heard Island glaciers over this period. Glacier change during the more recent investigated period was dramatic and unprecedented for the eastern facing glaciers on Heard Island - they declined by 30% or −1.0% yr^{-1} between 1988-2019.
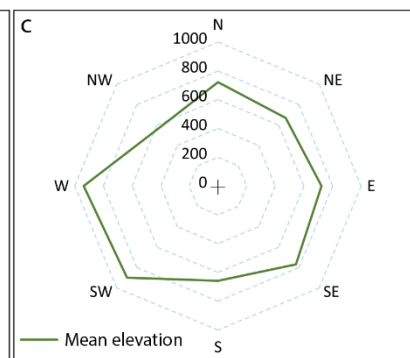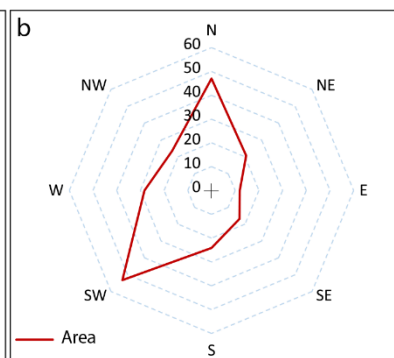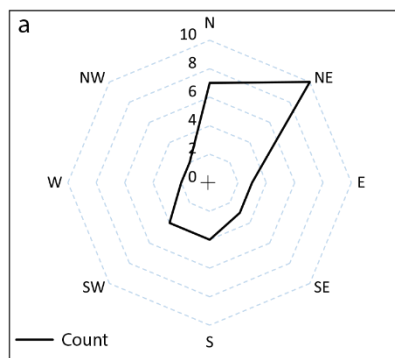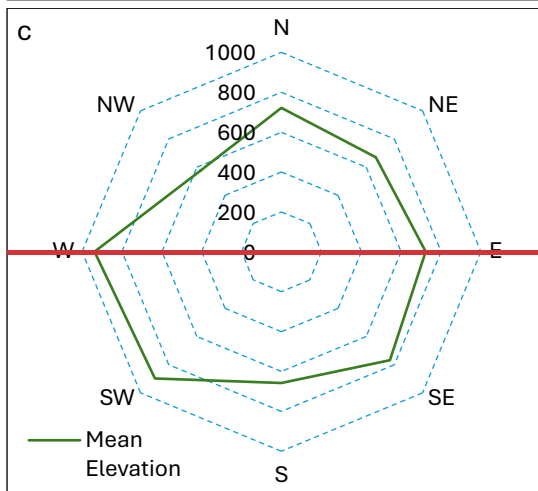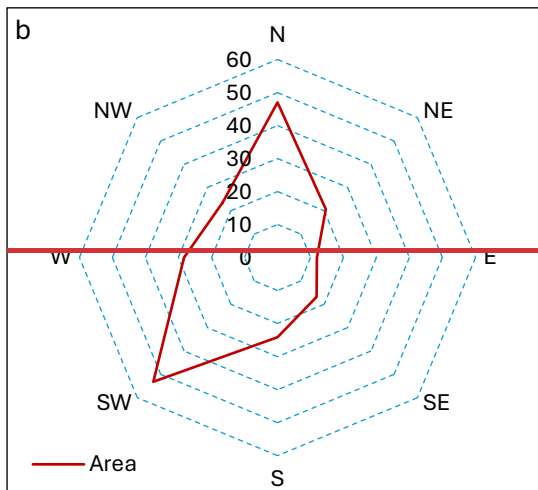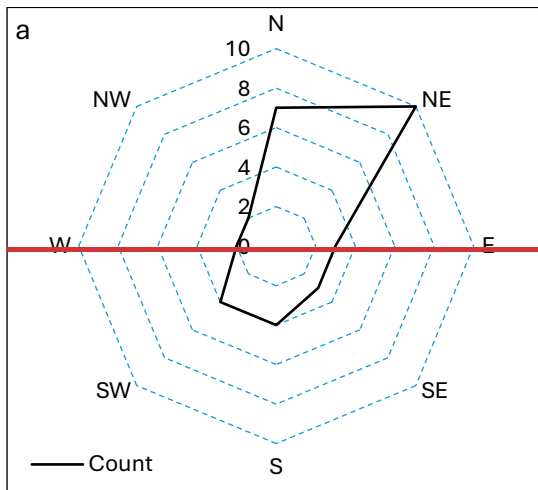
 Figure 56. Distribution of Heard Island glacier aspects by (a) number, (b) area (km^2) and
(c) mean elevation (a.s.l.) in 2019.

5.2 Glacier length changes

Brown and Stephenson glaciers showed significant terminus retreat, as evidenced by glacier shrinkage during the study period. Average total terminus retreat of 1483±20 m was observed for Brown Glacier between 1947–2019 with an annual mean retreat rate of −20.6 m yr^{-1} (Figure 6a). The retreat rate of −25.7 m yr^{-1} was much higher during the second investigated period (1988-2019).
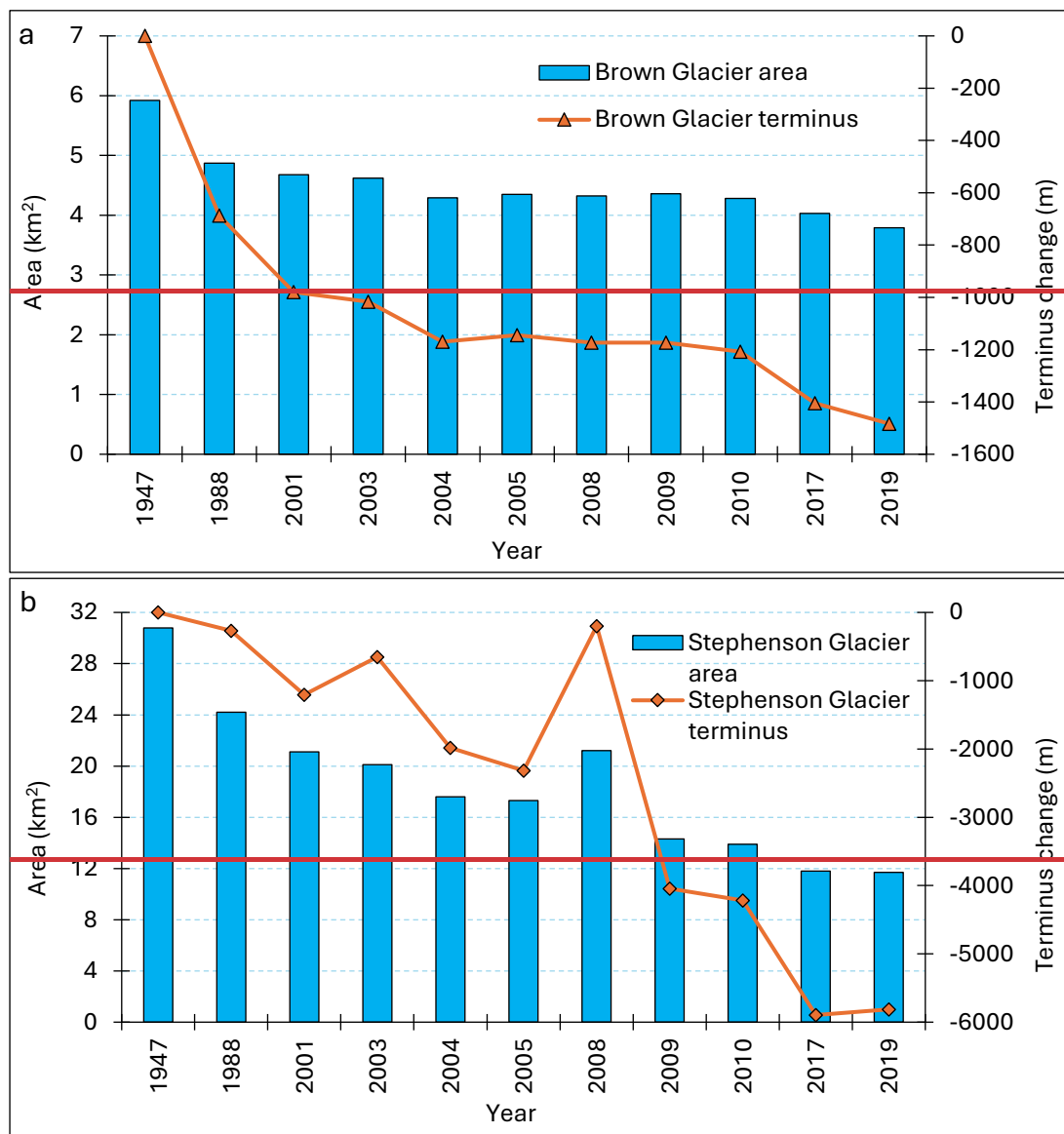
Figure 6. Cumulative terminus and area changes for Brown (a) and Stephenson (b) glaciers between 1947 and 2019.

Stephenson Glacier retreated more than any other glacier on Heard Island during our study period. The glacier terminus retreated by 5811±20 m between 1947–2019 yielding an annual retreat rates of −80.7 m yr⁻¹ (Figure ~~6~~7~~b~~). ~~Despite experiencing small readvances or relatively stable positions during some years, this didn't compensate for the massive overall retreat during this 72-year period.~~ The highest retreat of ~~Stevenson~~ Stephenson Glacier ~~retreated by~~ with −5541±20 m were recorded during the more recent ~~retreat~~ period (1988-2019), corresponding to an annual retreat rate of −178.7 m yr⁻¹ which is seven times higher than it was observed for Brown Glacier during the same time ~~(Figure 6b). The largest readvance was in 2005-2008 when glacier terminus extended by 2118±20 m but this was followed by a larger retreat of −3846±20 m yr⁻¹ between 2008-2009 (Figure 7).~~ Observations in Stephenson Lagoon during the summer of 2008 revealed a dense concentration of icebergs drifting towards the ocean, creating the illusion of a glacier readvance. However, the upper section of the glacier tongue showed no ~~movement~~change. Although a small terminus retreat was recorded from 2008 to 2009, the primary change was the complete ~~dissipation~~loss of the floating icebergs by 2009 (Supplement …).

413
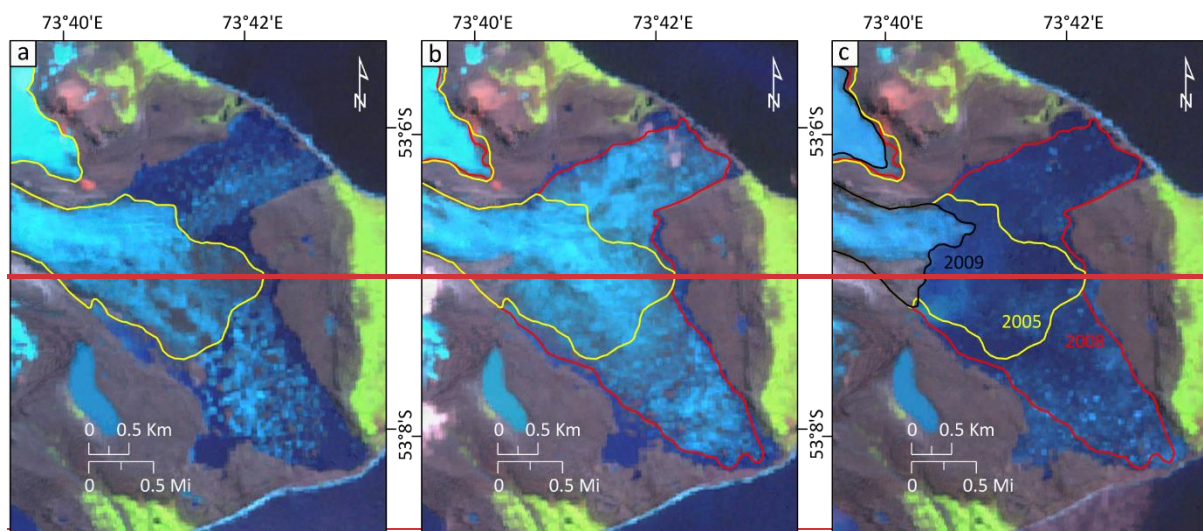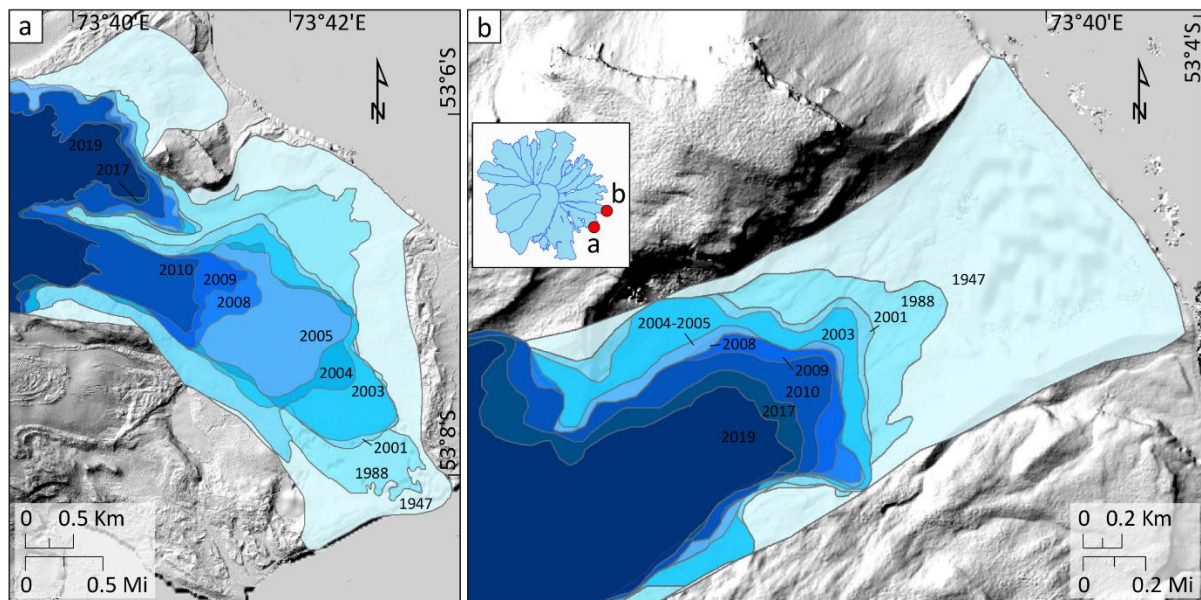
Figure 7. Stephenson (a) and Brown (b) Glacier ~~advance and~~ retreat ~~in~~ between ~~2005~~1947 and ~~2008–2009~~2019. ~~a – Landsat 7 ETM, 21/01/2005. b – Landsat 7 ETM, 04/02/2008. c – Landsat 7 ETM, 06/02/2009.~~ Pléiades Hillshade is used as a background (07/04/2019). Insert map on panel b shows location of the selected glaciers relative to other glaciers.

5.3 Surface debris cover changes in 1988-2019

We found that surface debris cover increased for all glaciers on Heard Island except those facing northwest and for glaciers on the Laurens Peninsula. Overall debris cover increased from 18.2±1.1 km^2 in 1988 to 29.0±1.6 km^2 in 2019. This increase in debris-covered area occurred despite a large decrease in corresponding glacier area over this period. The change equates to an increase in the proportion of debris-covered surface area from 7.0±6.0 % in 1988 to 12.8±5.5 % in 2019 (Figure 8).

The mean upper limit (or maximum elevation) of the debris cover shifted from 285±20 to 605±20 m a.s.l. between 1988 and 2019 for all debris-covered glaciers on Heard Island. The mean elevation of debris-covered parts also moved upwards from 165±20 to 410±20 m a.s.l. during this time. Southwest-facing Gotley Glacier had the highest mean upper limit of surface debris cover with an elevation of 985±20 m a.s.l. Glaciers at Laurens Peninsula had a small debris cover in 1988 but had become debris-free by 2019.

434
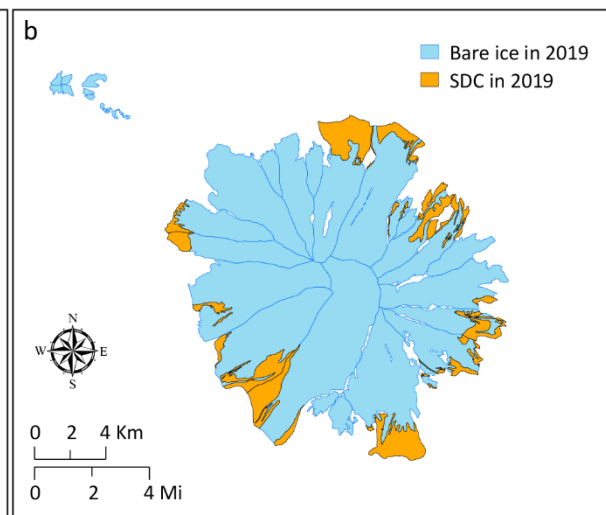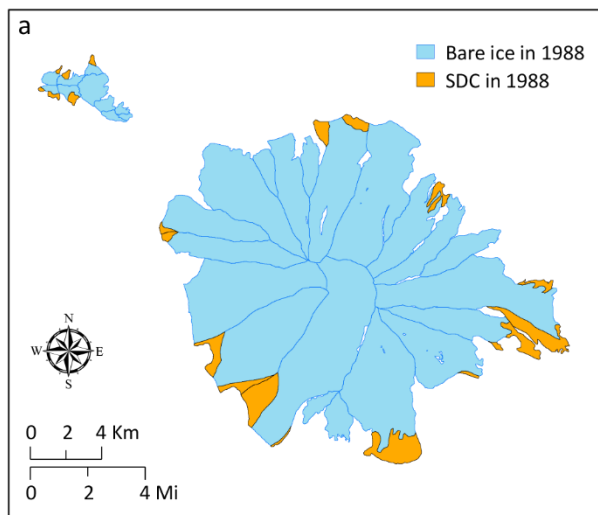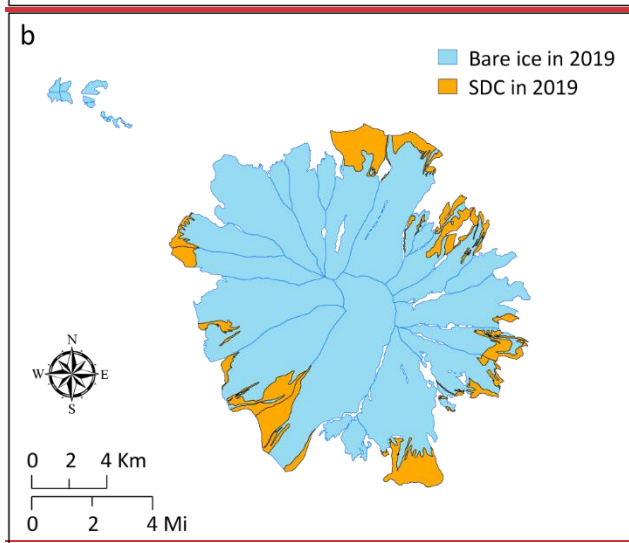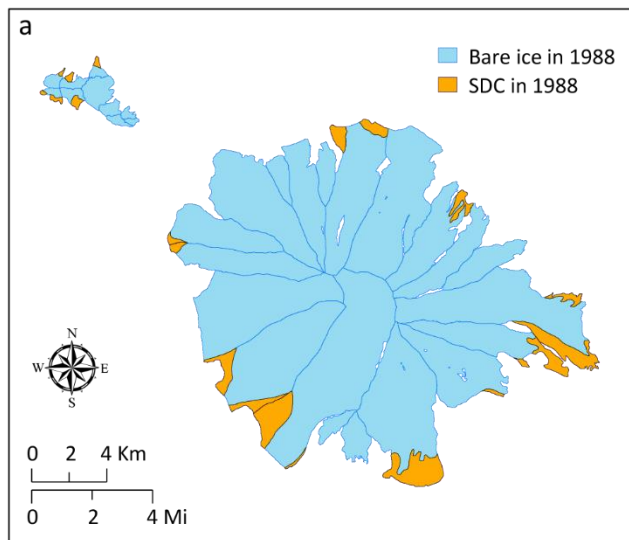
Figure 8. Decrease in bare ice and increase in surface debris cover (SDC) on Heard Island glaciers between 1988 (a) and 2019 (b).

6 Discussion

6.1 Glacier retreat and climate drivers

The relationship between climate and glacier changes in the Heard Island region must be considered cautiously because no local long-term weather station data are available. Instead, 2m surface air temperatures from ERA5 reanalysis (Soci et al., 2024) (0.5x0.5 deg) from a region encompassing Head Island (50-53° S, 70-73° E) were investigated between 1947 and 2019 (Figure 9). Comparison between the first (1947–1959) and last (2009–2019) decades show summer temperature (NDJFM) increase by 0.7 °C which is consistent with a previous record by Thost and Truffer (2008) who observed 0.8 °C increase of the summer temperatures between the 1948–1955 and 1997–2005 epochs. As shown in Figure ~~9a~~9, a warming trend of the mean annual summer temperatures and temperature anomalies relative to the long-term mean, specifically from the 1980s onwards, ~~is~~ also ~~aligns~~consistent with higher glacier retreat over the second investigated period, from the 1990s onwards.~~the increasing rate of glacier melting over the last 72 years. The period from 1980s onwards is particularly notable for increasingly frequent and extreme positive temperature anomalies relative to the long-term mean (Figure 9b).~~

Maritime glaciers such as those on Heard Island are particularly sensitive to air temperature changes (e.g. Anderson and Mackintosh, 2006; Davies et al., 2014). Warming causes the frequent precipitation to fall as rain rather than snow~~, decreasing surface albedo over the glaciers and leading to increased absorption of short-wave radiation and surface melt~~. ~~Warmer~~Higher temperatures also increase melt rates due to strong turbulent exchange in these windy environments (e.g. Anderson et al., 2010; Anderson and Mackintosh, 2012). For these reasons, the observed summer temperature increases ~~over the last 70 years~~since 1980s are likely an important driver of ongoing glacier recession on Heard Island. However, few precipitation measurements exist for Heard Island (Thost and Truffer, 2008), and Favier et al. (2016) showed that retreat of the Cook Ice Cap on the relatively nearby Kerguelen Islands is likely due to atmospheric drying since the 1960s rather than atmospheric warming. Further observations and modelling are required to ~~provide more~~increase confidence in our interpretation that climate warming was largely responsible for driving recent glacier retreat on Heard Island.

Our new glacier inventories indicate that Heard Island glaciers experienced ~~overall negative glacier mass balance~~higher area loss between 1988 and 2019. This finding is supported by satellite-based geodetic mass balance estimates for all Heard Island glaciers extracted from the global study of Hugonnet et al. (2021) (Figure 10). ~~However, a d~~Negative~~ifferent~~ mass balance ~~estimate~~values between 1990s and 2019, derived from a mixed method that incorporates in situ observations (Dussaillant et al., ~~2024~~2025) also aligns with higher glacier area loss from the 1990s onwards. ~~shows a~~A positive geodetic mass balance trend between 1976 and ~~1998~~1990s (Dussaillant et al., 2025), ~~maybe caused by~~perhaps due to a serious of relatively ~~low temperature~~cooler years ~~records during the same time~~ (Figure 9), ~~which is in~~ contrast~~s~~ ~~to~~with our observed glacier area reduction during the same period. This mismatch (Figure 10) could be for several

480 reasons: it might be because the glacier response is lagged and is responding to earlier
481 warming. Or it could be simply a function of data limitations including a~~is likely due to the~~
482 lack of direct mass balance observations to constrain the estimates of Dussaillant et al.
483 (~~2024~~2025)~~,~~ ~~as well as the lack of the~~ and limited instrumental meteorological
484 observation in this remote region to ~~corelate with~~support the ERA5 dataset.

485 The warming trend evident in ERA5 data in the Heard Island region (0.7°C) is relatively
486 small to the observed 1.1°C warming for the neighbouring Kerguelen Island between
487 1951-2020 (Nel et al., 2023) but it is in agreement with general Southern Ocean warming
488 trend since 1950s (Auger et al., 2021; Li et al., 2023). The primary driver of atmospheric
489 and ocean warming in this region is ~~the~~ a human-induced shift towards the positive phase
490 of the Southern Annular Mode (Pohl et al., 2021), ~~which has caused~~associated with an
491 intensification and poleward shift of the Southern Hemisphere westerly winds (Perren et
492 al., 2020). ~~Further accelerated decline in ice cover and warming air temperatures in the~~
493 ~~Heard Island region mean that the glaciers may be rapidly approaching an irreversible~~
494 ~~tipping point in the sub-Antarctic (Bakke et al. 2021), impacting landscape, geomorphic~~
495 ~~and ecosystem processes.~~

496 Volcanic activity is another potential factor that could be contributing to the accelerated
497 glacier melting on Heard Island. Glacier ~~retreat might~~mass loss also be a trigger for
498 enhanced volcanism at Heard Island due to decompression of the underlying magma
499 chamber (e.g. Barr et al., 2018). Eruptions could cause significant melting of the ice or
500 deposition of the thin layer of tephra, while increases in geothermal heat may lead to
501 greater basal melting, thereby influencing glacier movement (Allison and Keage, 1986;
502 Fox et al., 2021). Conversely, sufficiently thick deposition of tephra on glacier surface
503 might also decrease glacier mass loss (Kirkbride and Dugmore, 2003). However, given the
504 lack of direct evidence in satellite images for unusual melt or tephra cover, the fact that
505 accelerated glacier melt occurred on all Heard Island glaciers and not just a subset, and
506 also on nearby Kerguelen Islands (Berthier et al., 2009; Deline et al., 2024), we consider
507 that any volcanic drivers of glacier retreat are less important than climatic ones.

508
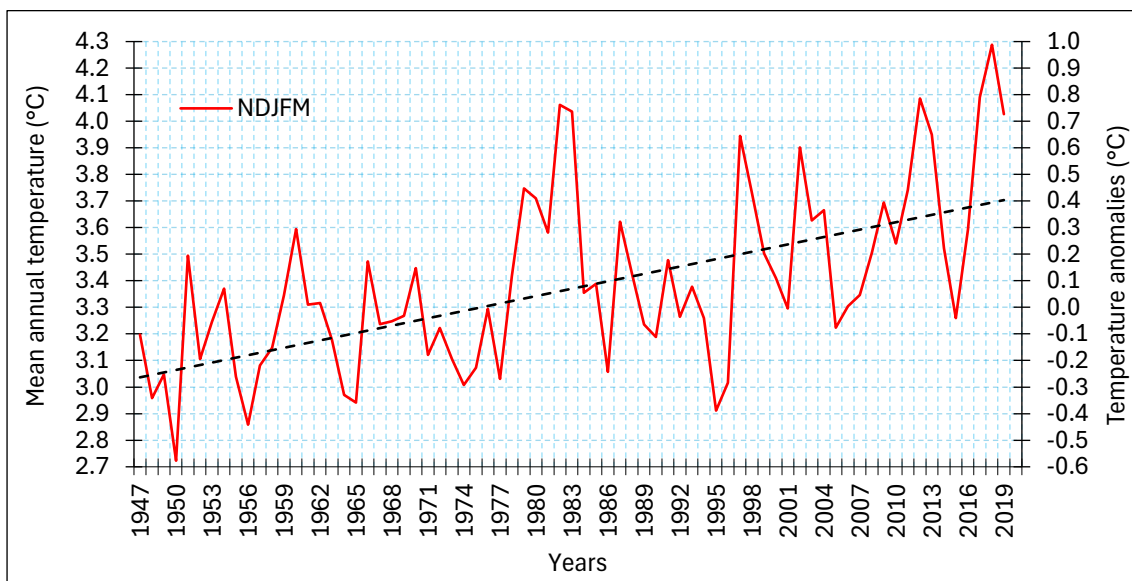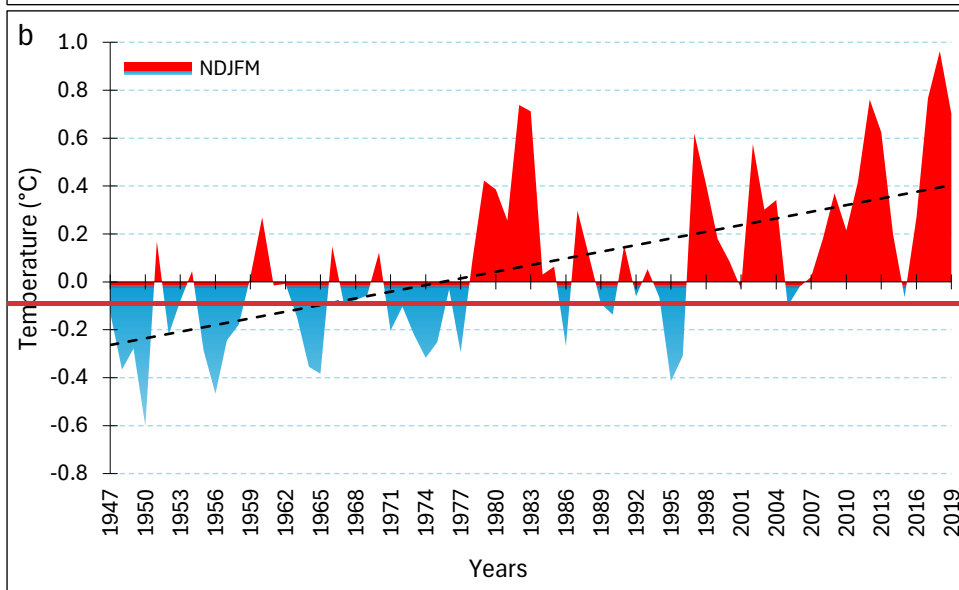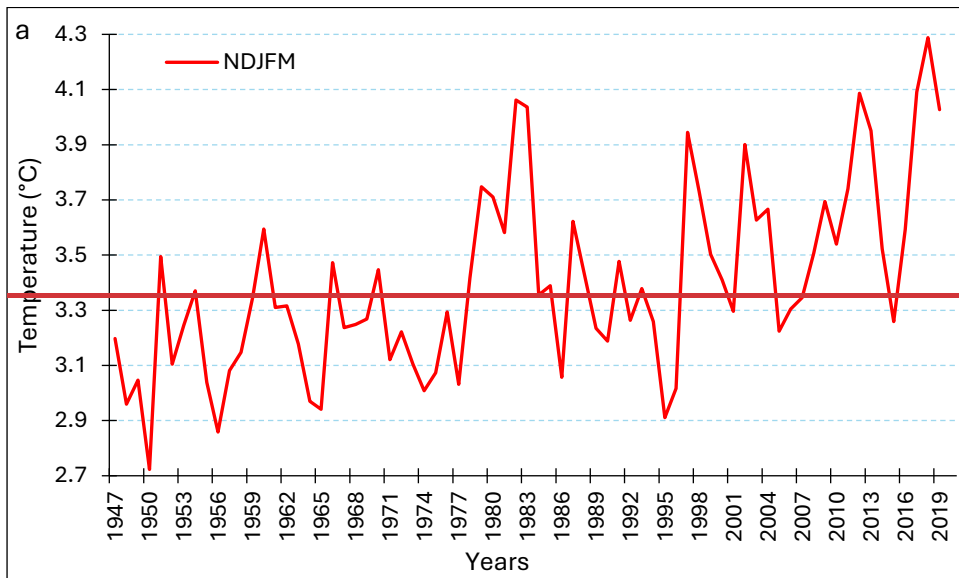
Figure 9. ~~a -~~ Mean annual warm season (NDJFM) temperatures and monthly air temperature anomalies (°C) for Heard Island between 1947-2019. ~~b - Time series of warm~~

season (NDJFM) monthly air temperature anomalies for the same period. The black dashed line ~~on panel 'b'~~ is the trend showing a warming rate of 0.7 °C over time. Both ~~panels~~ values are based on the ERA5 2 m surface air temperature dataset.
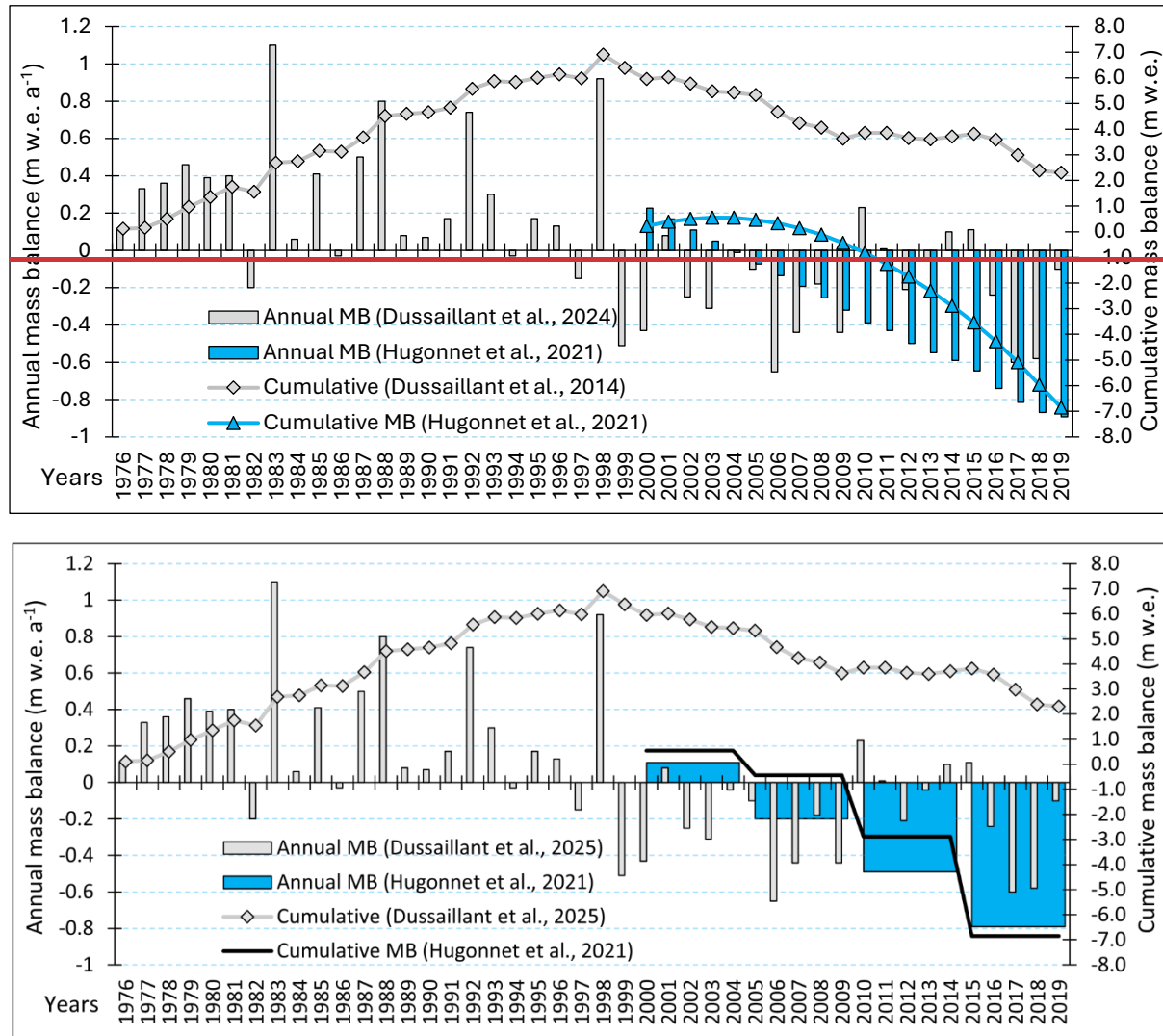
Figure 10. Mean annual geodetic mass balance (m w.e. a⁻¹) and cumulative mass balance (m w.e.) for all Heard Island glaciers between 2000-2019 (Hugonnet et al., 2021) (averaged within a rolling window of 5 years) and between 1976–2019 (Dussaillant et al., ~~2014~~2025).

6.2 The role of aspect and glacier lake formation on glacier retreat

We observed that higher rates of glacier retreat occurred on the eastern side of the island (Figure 3). Although climate data are ~~sparce~~ sparse and a process-based modelling approach is required for further investigation, we expect this greater sensitivity of east-facing glaciers is due to ~~factors such as increased foehn winds~~orographic effects;

satellite observations and limited climate station data show that the eastern side of the island, in the lee of the prevailing westerly winds, is less cloudy, warmer and receives less precipitation.(and correspondingly warmer air temperatures) and reduced precipitation on the downwind side of the island. This asymmetry has been noted inOur findings agree with previous studies of Heard Island glaciers (e.g. Thost and Truffer, 2008) and is consistent with other islandsstudies in the sub-Antarctic region where strong westerly winds interact with mountain barrierswhich show a similar asymmetry. For example, Berthier et al. (2009) observed that the eastern part of Cook Ice Cap on Kerguelen shrank 2.5 times more (~28%) than the western part (~11%) between 1963 and 2003. Similar observations have been made in South Georgia, where glacier decrease on the east coast was higher than on the windy and wet southwest coast during the second half of the 20th century (Gordon et al., 2008).

Comparison with other glacier retreat records from the southern mid to high latitudes (Figure 11) shows that lake formation is a key driver of accelerated glacier retreat. Brown Glacier on Heard Island initially experienced rapid retreat as a proglacial lake formed between 1947 and 1988; this is like Chamonix Glacier on Kerguelen which initially retreated in a lake but has been land terminating for several decades subsequently. The retreat rate of these glaciers once they become land-terminating is relatively linear. and similar to the retreat rate of the land-terminating Fox and Franz Josef Glaciers in New Zealand (Purdie et al., 2020; Mackintosh et al., 2017) (Figure 11).

In contrast, Stephenson Glacier on Heard Island is notable for its unprecedentedly high terminus retreat, particularly –between 1988 and 2019 when the glacier retreated by almost 5.5. km compared to 0.8 km at Brown Glacier (Figure 11). Lake formation at Stephenson Glacier was much later than at Brown, and once a proglacial lake did form it became extremely large. This is like the situation at Agassiz Glacier on Kerguelen which retreated into its proglacial lake more recently than Chamonix Glacier (Deline et al., 2024), and also Tasman Glacier in New Zealand which retreated more than 4.5 km in its proglacial lake over recent decades (Mackintosh et al., 2017; Purdie et al., 2020).
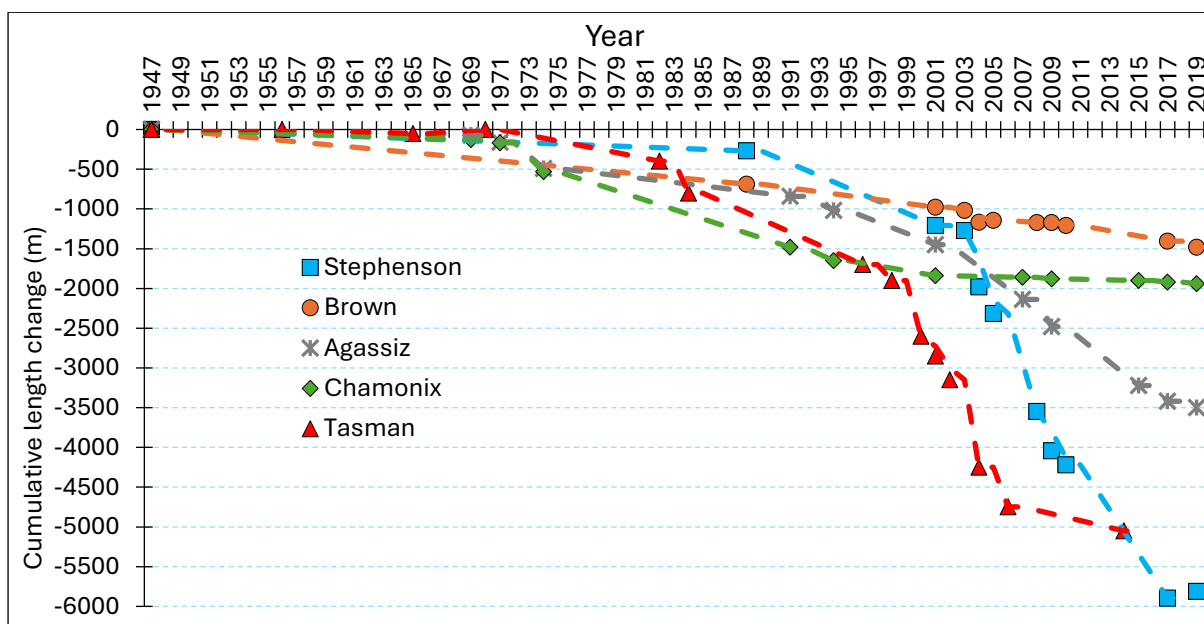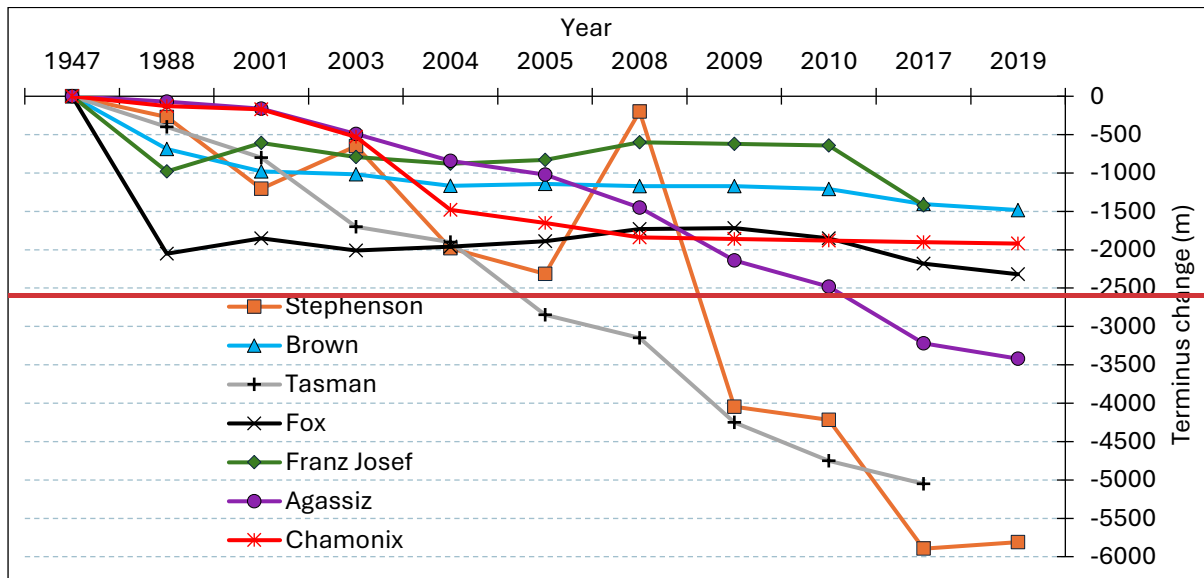
Figure 11. Cumulative ~~terminus~~ length changes between 1947–2019 for Brown and Stephenson glaciers (current study) compared to Agassiz and Chamonix glaciers on Kerguelen (Deline et al., 2024) and ~~Fox, Franz Josef and~~ Tasman ~~glaciers~~ Glacier in New Zealand (Purdie et al., 2020; Mackintosh et al., 2017).

The retreat of Stephenson Glacier warrants further discussion. In the 1950s, the glacier had a steep and small accumulation area relative to its long (~5.5 km) and low angle terminus compared to its counterparts~~. and a~~ A significant portion of that tongue was located near sea level (Figure 12). This is due to the subtle and flatter topography of eastern lower part of Heard Island (see also Figure 1c). This steep/small accumulation area, low angle terminus, relatively high ablation rates at sea level and melting by seawater and mechanical calving by tidal action (Truffer and Motyka, 2016) likely made the glacier more susceptible to warming. Once lagoon formation initiated, the high

retreat rate of the Stephenson Glacier was enhaced by calving as the glacier retreated into its overdeepend basin.~~Low angle glaciers are particularly sensitive to climate change (e.g. Oerlemans, 2001) and those that terminate at sea level are subject to rapid surface and subaqueous ablation throughout the year due to warm air temperatures and melting by seawater and mechanical calving by tidal and wave action (Truffer and Motyka, 2016). Therefore, we propose that, along with increased air temperatures, the high retreat rate of the Stephenson Glacier may be related to the low topography and flat surface of the glacier tongue and the negative impact of the very large lagoon connected to ocean water.~~ We also note that despite recent efforts to quantify ~~ocean~~ water properties in similar environments (Mortensen et al., 2013; Straneo and Cenedese, 2015), rates of subaqueous melting for Heard Island glaciers along with the water properties of the associated lagoons are largely unknown and require further investigation. ~~Finally, the small readvances observed at Stephenson's Glacier are also characteristic of tidewater glaciers which can undergo non-climatic advance and retreat cycles (Vieli, 2011).~~
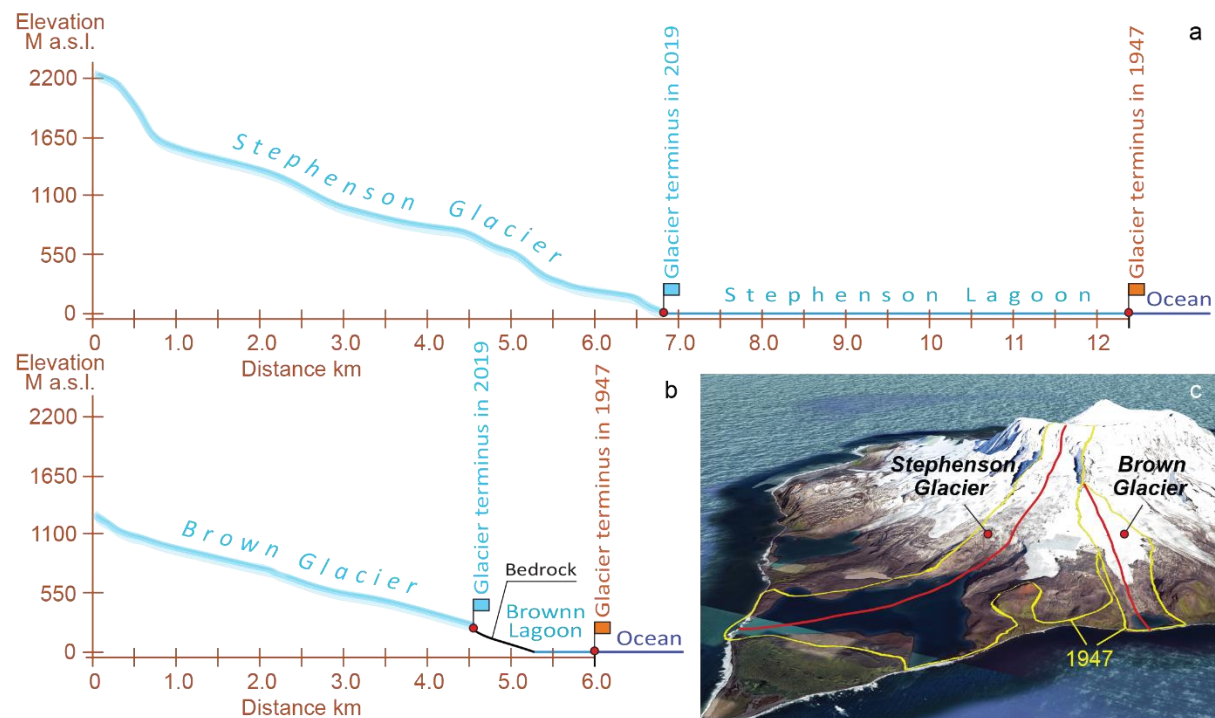
Figure 12. Longitudinal profiles based on Pléiades DSM, 2019. a – Stephenson Glacier; b – Brown Glacier; c – Longitudinal profile paths (in red) for both glaciers on 3D view (© Google Earth).

6.3 Evolution of Surface Debris Cover in 1988-2019~~Impact of surface debris cover on glacier retreat~~

It is widely ~~confirmed~~observed that in glacio-volcanic regions, volcanic eruptions regularly deposit tephra onto adjacent glaciers (Nield et al., 2013). These deposits into

the ice system produces a significant component of the surface debris ~~pattern of glacial lobes draining~~on these ice masses (Kirkbride and Dugmore, 2003). Ash-ice interactions can significantly modulate glacial mass balance responses to climatic changes, affecting glaciers for decades following eruptions (e.g. Richardson and Brook, 2010; Rivera et al., 2012). Given Heard Island's glacio-volcanic nature, we consider both rock fall and tephra deposition, or a combination, as possible debris cover sources.

Despite an overall increase since 1988, surface debris has varied between individual glaciers and some glaciers have contradicted the overall trend. e.g. ~~A~~ a substantial amount of surface debris cover was found on Stephenson Glacier in 1988 (~14%), mainly near the terminus, which had almost disappeared by 2019 (~2.9%). This could be because the glacier still had a low-angle tongue in 1988 that was favourable for debris accumulation (e.g. Mölg et al., 2019), but that this debris-laden ice subsequently calved into the lake. ~~The debris cover at Stephenson Glacier prior to 1988 may have contributed to the accelerated terminus retreat if debris was less than a few cm thick, as this would have led to enhanced surface melting (e.g. Östrem, 1959). However, surface debris thickness and properties have not been measured at Heard Island and this inference is speculative.~~

The most significant increase of surface debris cover was observed on northeast facing Downes Glacier from ~9.8% in 1988 to ~31.6% in 2019, while the total area of this glacier has only reduced by ~4.3% during the same period (Figure ~~3~~4, 8). It is not clear what drove this increase (Figure 13). ~~, though the lack of bare cliffs above the glacier (Figure 13) suggests a subglacial source.~~ However, as our debris cover trends are derived from only two satellite images, the differences in debris-covered area might only be related to different snow conditions rather than a real increase (e.g. if the snow line in 1988 was lower). More investigation is needed as there is no obvious ~~clear~~ process that can account for the observed development of surface debris cover at Downes Glacier relative to other glaciers on Heard Island.
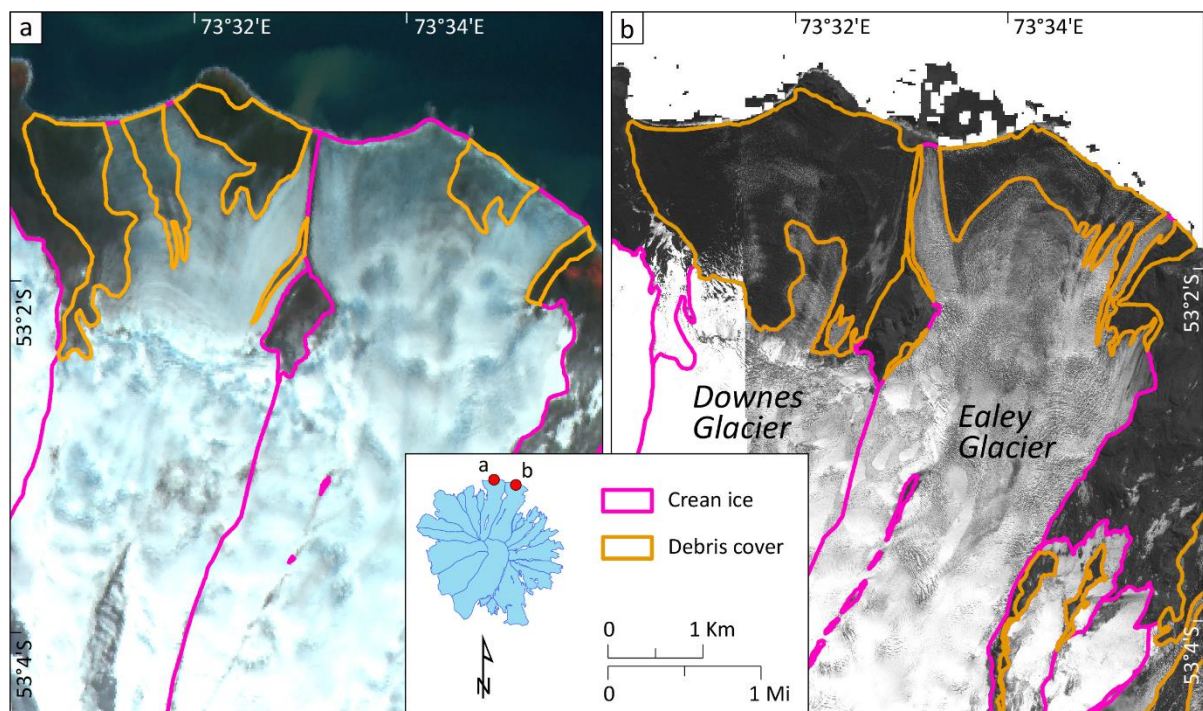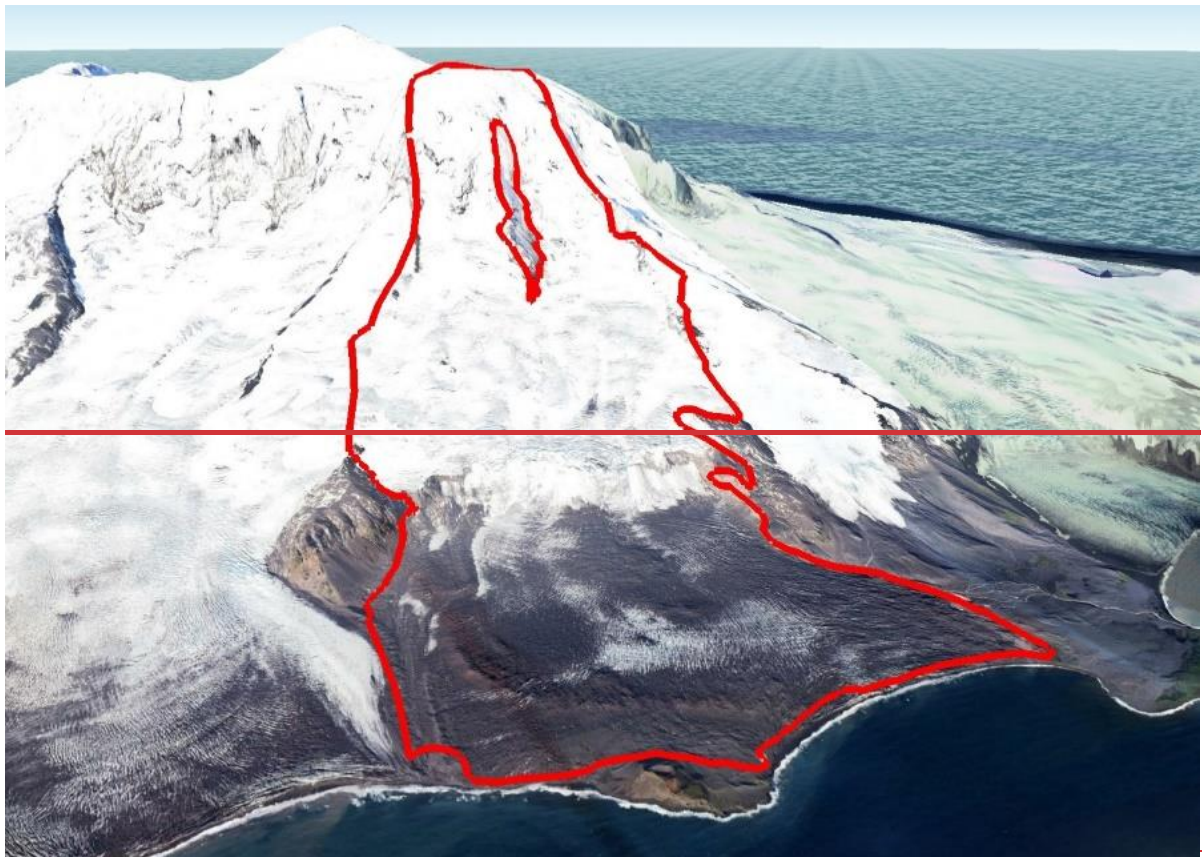
Figure 13. The most heavily debris-covered Downes Glacier along with Ealey Glacier within the Heard Island. a – 1988; b – 2019. (SPOT_1 (09/01/1988) and Pléiades ortho image (07/04/2019) is used as a background31/03/2024 © Google Earth). Insert map into the legend shows location of the selected glaciers relative to other glaciers.

6.4 Comparison with previous studies

The GLIMS book (Kargel et al., 2014) estimated 29 glaciers on Heard Island with a cumulative area of 257 km^2 based on SPOT image from 1988 (Cogley et al., 2014), while the Randolph Glacier Inventory (RGI v6 and v7) database identifies 31 glaciers with a total area of 254.4 km^2 (Pfeffer et al., 2014; Maussion et al., 2023) based on same SPOT image from 1988. Both estimates fit within the uncertainty of our assessment 260.3±6.3 km^2 in 1988. However, glaciers in RGI v6 and v7 databases are characterized with inaccurate ice margins (due to misidentification of ice divides), which have been rectified after this in our inventory (Figure 14).
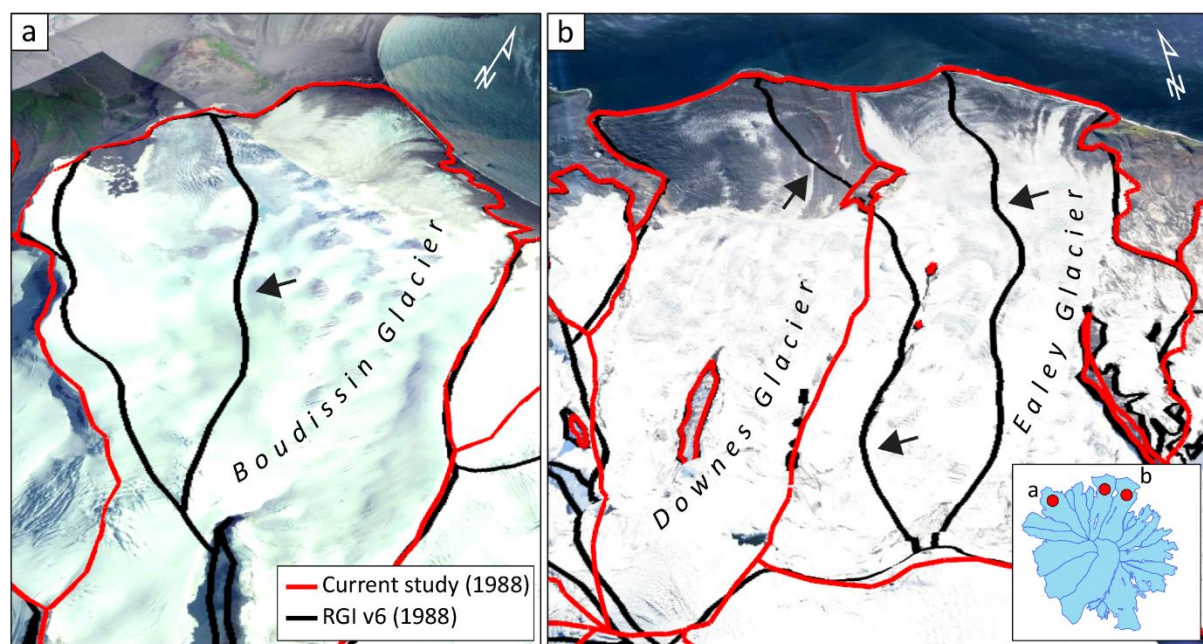
Figure 14. Comparison of RGI v6-v7 (Pfeffer et al., 2014; Maussion et al., 2023) to current study for the Boudissin Glacier (a) and Downes/Ealey glaciers (b). Black arrows show inaccurate ice margins in RGI v6-v7 (due to misidentification of ice divides).

A global assessment of surface debris cover by Scherler et al. (2018) uses residual between RGIv6 outlines (which include manually mapped debris-cover) and an automatically digitizsed clean ice map. for Heard Island delineated based on Spot images from 1988. We extracted these outlines from Scherler et al. (2018) for our glacier sample from 1988 to compare results (Figure 1415). We found that Scherler et al. (2018) reported much higher percentage (25.2 %) of surface debris cover for Heard Island than our study (7.0 %) in 1988. This does not even match fit within our uncertainty (±6.0 %). These differences are probably explained by automatized method of global assessment of surface debris coverclean ice by Scherler et al. (2018). E.g. Common problems in ice-cover mapping from optical imagery are related to shadows as well as cloud and snow cover and manual corrections are required (e.g. Paul et al., 2013), while Ourour approach

660 only uses accurate manual digitization., while automated mapping often fails and
661 manual corrections are required (e.g. Paul et al., 2013).

662

663
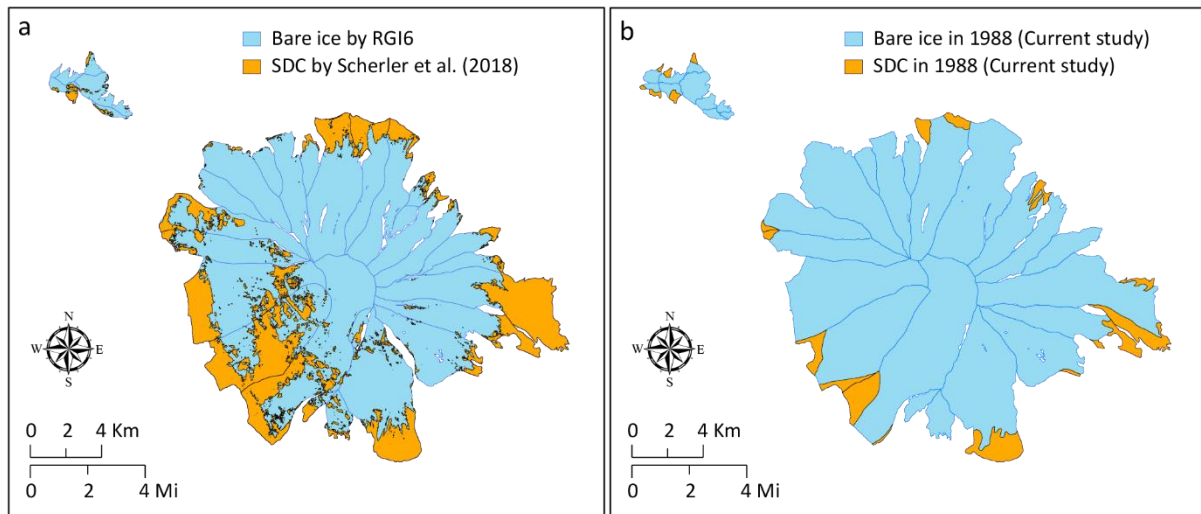
664 **Figure 1415**. a – extracted surface debris cover (SDC) data from Scherler et al. (2018).
665 Glacier outlines from RGIv6 from 1988; b – SDC from our study from 1988.

666

7 Conclusions

668 We present a multi-year glacier inventory based on historic topographical maps,
669 highmedium-, and very high-resolution satellite imagery and digital elevation/surface
670 models. Our findings show that glaciers on Heard Island experienced significant area loss
671 (22% or −0.31% yr^{-1}) over the 72-year period between 1947-2009, from 289.4±6.1 km^2 to
672 225.7±4.2 km^2 with an increasing rate of ice loss in recent decades. Our study also shows
673 that the small and low elevation glaciers at Laurens Peninsula have experienced the
674 highest recession rates of −1.1% yr^{-1} over the last 72 years.

675 We observed much higher glacier area decrease and terminus retreat on the east and
676 southeast side of Heard Island. We suggest that this difference results from topographic
677 influences on the island's climate as well as its glaciers; orographic processes lead to a
678 warmer and drier climate on the eastern side of the island, and the low-angle glacier
679 termini are more susceptible toAlthough this asymmetry may have an underlying climate
680 driver, for example due to increased foehn winds, topographic factors have clearly played
681 a role; ice retreat on the eastern side of the island has been enhanced at low-elevation
682 and low-angle tongues where glaciers have transitioned from land based to lake calving.
683 Stephenson's Glacier is an exemplar of this behaviour. Surface debris cover has also
684 increased on most Heard Island glaciers and could also be a contributor to accelerating
685 ice loss.

686 Our new glacier inventory for Heard Island tracks changes in glacier extent, and
687 dynamics, providing insights into the impact of climate change in this remote and

sensitive region. Further work is required to test some of the ideas we have put forward in this paper regarding the different roles of climatic and non-climatic factors in driving ice retreat. The new inventory will also help to better understand how changes in glaciers affect biodiversity and ecosystems, which will inform conservation and management efforts at this World Heritage site.

Data availability

~~Will~~ Glacier outlines will be submitted to GLIMS (https://www.glims.org/) and can be used for future studies.

Supplement

Heard Island Glacier Inventory includes satellite image screenshots (Landsat 7 ETM+ panchromatic bands) for the Stephenson Glacier terminus between 2001 and 2010. The supplement related to this article is available online at: https://doi.org/......

Author contributions

LGT and ANM designed the conceptual framework for the study. LGT mapped glacier outlines and led the scientific interpretation and writing, with contributions from ANM and WY.~~wrote the paper with input and feedback from ANM and WY.~~

Competing interests

The contact author has declared that neither they nor their co-authors have any competing interests.

Acknowledgements

Medium-resolution SPOT and high-resolution Pléiades images acquired by French Space Agency (CNES)'s Spot World Heritage Programme and Pléiades Glacier Observatory. We are very grateful to Dr Etienne Berthier for his help in obtaining the satellite images. We would like to thank Dr Frank Paul and the anonymous reviewer for their thoughtful and constructive comments, which clearly ~~enhanced the quality of~~improved the manuscript.

Financial support

This work was supported by the Australian Research Council (ARC) Special Research Initiative (SRI) Securing Antarctica's Environmental Future (SR200100005).

References

722

723 **References**

724 Allison, I. F.: A preliminary investigation of the physical characteristics of the Vahsel
725   Glacier, Heard Island. ANARE Scientific Reports Series A(4); Glaciology. Publication
726   128. Canberra, Australian Government Publishing Service, 1980.

727 Allison, I. F., and Keage, P. L.: Recent changes in the glaciers of Heard Island. Polar
728   Record. 23(144):255-272. https://doi.org/doi:10.1017/S0032247400007099, 1986.

729 Allison, I., and Thost, D. E.: Heard Island glacier fluctuations and climatic change.
730   Australian Antarctic Data Centre. data.aad.gov.au/metadata/records/ASAC_1158,
731   2000.

732 Anderson, B., Mackintosh, A., Stumm, D., George, L., Kerr, T., Winter-Billington, A., and
733   Fitzsimons, S.: Climate sensitivity of a high-precipitation glacier in New Zealand.
734   Journal of Glaciology, 56(195), 114-128.
735   https://doi.org/doi:10.3189/002214310791190929, 2010.

736 Anderson, B., and Mackintosh, A.: Temperature change is the major driver of late-glacial
737   and Holocene glacier fluctuations in New Zealand. Geology; 34 (2): 121–124. doi:
738   https://doi.org/10.1130/G22151.1, 2006.

739 Anderson, B., and A. Mackintosh.: Controls on mass balance sensitivity of maritime
740   glaciers in the Southern Alps, New Zealand: The role of debris cover, J. Geophys.
741   Res., 117, F01003, https://doi.org/doi:10.1029/2011JF002064, 2012.

742 Aubert de la Rue, E.: "Un Voyage d'exploration dans les mers Australes. Iles Heard,
743   Archipel de Kerguelen, ile St. Paul."" Rev. de Geogr. Phys. et de Geol. Dynam. Univ.
744   de Paris, 11, 97-146, 1929.

745 Auger, M., Morrow, R., Kestenare, E. et al.: Southern Ocean in-situ temperature trends
746   over 25 years emerge from interannual variability. Nat Commun 12, 514.
747   https://doi.org/10.1038/s41467-020-20781-1, 2021.

748 Bakke, J., Paasche, Ø., Schaefer, J. M. and Timmermann, A.: Long-term demise of sub-
749   Antarctic glaciers modulated by the Southern Hemisphere westerlies. Scientific
750   Reports, 11, 10.1038/s41598-021-87317-5, 2021.

751 Barr, I. D., Lynch, C. M., Mullan, D., De Siena, L., and Spagnolo, M.: Volcanic impacts on
752   modern glaciers: A global synthesis. Earth-Science Reviews Vol., 182, 0012-8252,
753   https://doi.org/10.1016/j.earscirev.2018.04.008, 2018.

754 Berthier, E., Le Bris, R., Mabileau, L., Testut, L. and Rémy, F.: Ice wastage on the Kerguelen
755   Islands (49°S, 69°E) between 1963 and 2006. J. Geophys. Res. 114, F03005,
756   https://doi.org/10.1029/2008JF001192, 2009.

Berthier, E., Lebreton, J., Fontannaz, D., Hosford, S., Belart, J. M.-C., Brun, F., Andreassen, L. M., Menounos, B., and Blondel, C.: The Pléiades Glacier Observatory: high-resolution digital elevation models and ortho-imagery to monitor glacier change, The Cryosphere, 18, 5551–5571, https://doi.org/10.5194/tc-18-5551-2024, 2024.

Bolch, T., Menounos, B., and Wheate, R.: Landsat-based inventory of glaciers in western Canada, 1985–2005, Remote Sens. Environ., 114, 127–137, https://doi.org/10.1016/j.rse.2009.08.015, 2010.

Bosson, J. B., Huss, M., Cauvy-Frraunié, S., Clément, J. C., Costes, G., Fischer, M., Poulenard, J. and Arthaud, F.: Future emergence of new ecosystems caused by glacial retreat. Nature 620, 562–569. https://doi.org/10.1038/s41586-023-06302-2, 2023.

Bhambri, R., Bolch, T., Chaujar, R. K., Kulshreshtha, S. C.: Glacier changes in the Garhwal Himalaya, India, from 1968 to 2006 based on remote sensing. Journal of Glaciology. 57(203):543-556. https://doi.org/doi:10.3189/002214311796905604, 2011.

Budd, G. M.: Heard Island Expedition, 1963. Polar Record. 1964; 12(77):193-195. https://doi.org/doi:10.1017/S0032247400054619, 1964.

Budd, G. M.: Heard Island Reconnaissance, 1969. Polar Record. 1970;15(96):335-336. https://doi.org/doi:10.1017/S0032247400061131, 1970.

Budd, G. M. and Stephenson, P. J.: Recent glacier retreat on Heard Island. In Gow, A. J. and others (editors). Proceedings of the International Symposium on Antarctic Glaciological Exploration, Hanover NH, 1968: 449–58. IAHS Publication 86, 1970.

Budd, G. M.: Changes in Heard Island glaciers, king penguins and fur seals since 1947. Papers and Proceedings of the Royal Society of Tasmania, vol. 133, no. 2, pp. 47-60, https://doi.org/10.26749/rstpp.133.2.47, 2000.

Burgess, D. O., and Sharp, M. J.: Recent Changes in Areal Extent of the Devon Ice Cap, Nunavut, Canada. Arctic, Antarctic, and Alpine Research, 36(2), 261–271. https://doi.org/10.1657/1523-0430(2004)036[0261:RCIAEO]2.0.CO;2, 2004.

Cogley, J. G., Berthier, E., Donoghue, S.: Remote Sensing of Glaciers of the Subantarctic Islands. In: Kargel, J., Leonard, G., Bishop, M., Kääb, A., Raup, B. (eds) Global Land Ice Measurements from Space. Springer Praxis Books. Springer, Berlin, Heidelberg. https://doi.org/10.1007/978-3-540-79818-7_32 , 2014.

Davies, B., Golledge, N., Glasser, N. et al.: Modelled glacier response to centennial temperature and precipitation trends on the Antarctic Peninsula. Nature Clim Change 4, 993–998. https://doi.org/10.1038/nclimate2369, 2014.

DeBeer, C. M., and Sharp, M, J.: Recent changes in glacier area and volume within the southern Canadian Cordillera. Annals of Glaciology. 46:215-221. https://doi.org/10.3189/172756407782871710, 2007.

Deline, P., Linge, H., Ravanel, L., et al.: Mapping of morainic complexes and reconstruction of glacier dynamics north-east of Cook Ice Cap, Kerguelen Archipelago (49°S). Antarctic Science. 36(2):75-100. https://doi.org/10.1017/S0954102023000378, 2024.

Division of National Mapping.: Topographic map of Heard Island. Scale 1:50,000. MAP G9182.H4. Produced by the Division of National Mapping, Dept. of National Development. https://nla.gov.au/nla.obj-2545184819, 1964.

Drygalski, E. Von: "Geogr. von Heard Eiland.'? Deutsche Sudpolar Exped., 1901-3. Bd. 11, Heft 3. Geog. u. Geol. 223-39, 1908.

Dussaillant, I., Hugonnet, R., Huss, M., Berthier, E., Bannwart, J., Paul, F., and Zemp, M.: Annual mass changes for each glacier in the world from 1976 to 2023, Earth Syst. Sci. Data Discuss. [preprint], https://doi.org/10.5194/essd-2024-323, in review, 2024.

Eis, J., van der Laan, L., Maussion, F., and Marzeion, B.: Reconstruction of Past Glacier Changes with an Ice-Flow Glacier Model: Proof of Concept and Validation. Front. Earth Sci. 9:595755. https://doi.org/10.3389/feart.2021.595755, 2021.

Favier, V., Verfaillie, D., Berthier, E. et al.: Atmospheric drying as the main driver of dramatic glacier wastage in the southern Indian Ocean. Sci Rep 6, 32396. https://doi.org/10.1038/srep32396, 2016.

Fox, J. M., McPhie, J., Carey, R. J., Jourdan, F., and Miggins, D. P.: Construction of an intraplate island volcano: The volcanic history of Heard Island. Bull Volcanol 83, 37. https://doi.org/10.1007/s00445-021-01452-5, 2021.

Freudiger, D., Mennekes, D., Seibert, J., and Weiler, M.: Historical glacier outlines from digitized topographic maps of the Swiss Alps, Earth Syst. Sci. Data, 10, 805–814, https://doi.org/10.5194/essd-10-805-2018, 2018.

Gordon, J. E., V. M. Haynes, and A. Hubbard.: Recent glacier changes and climate trends on South Georgia, Global Planet. Change, 60(1–2), 72–84, https://doi.org/10.1016/j.gloplacha.2006.07.037, 2008.

Granshaw, F. D. and Fountain, A. G.: Glacier change (1958–1998) in the North Cascades National Park Complex, Washington, USA, J. Glaciol., 52, 251–256, https://doi.org/10.3189/172756506781828782, 2006.

Hall, D. K., Bayr, K. J., Schöner, W., Bindschadler, R. A., and Chien, J. Y. L.: Consideration of the errors inherent in mapping historical glacier positions in Austria from the ground and space (1893–2001), Remote. Sens. Environ., 86, 566–577, https://doi.org/10.1016/S0034-4257(03)00134-2, 2003.

HIMI (Heard Island and McDonald Islands) Marine Reserve Management Plan 2014-2024: Dep. of the Env. Canberra 22, http://heardisland.antarctica.gov.au/, 2014.

831 HIMI (Heard Island and McDonald Islands) official website.
832 https://www.antarctica.gov.au/antarctic-operations/stations/other-
833 locations/heard-island/climate-and-weather/ last access: August 2024.

834 Hock, R., Rasul, G., Adler, C., Cáceres, B., Gruber, S., Hirabayashi, Y., Jackson, M., Kääb,
835 A., Kang, S., Kutuzov, S., Milner, A., Molau, U., Morin, S., Orlove, B., and Steltzer, H.:
836 High Mountain Areas, in: IPCC Special Report on the Ocean and Cryosphere in a
837 Changing Climate, edited by: Pörtner, H. O., Roberts, D. C., Masson-Delmotte, V.,
838 Zhai, P., Tignor, M., Poloczanska, E., Mintenbeck, K., Alegría, A., Nicolai, M., Okem,
839 A., Petzold, J., Rama, B., and Weyer, N. M., 2019.

840 Hugonnet, R., McNabb, R., Berthier, E., Menounos, B., Nuth, C., Girod, L., Farinotti, D.,
841 Huss, M., Dussaillant, I., Brun, F., and Kääb, A.: Accelerated global glacier mass
842 loss in the early twenty-first century, Nature, 592, 726–731,
843 https://doi.org/10.1038/s41586-021-03436-z, 2021.

844 Huss, M., Hock, R.: Global-scale hydrological response to future glacier mass loss.
845 Nature Clim Change 8, 135–140. https://doi.org/10.1038/s41558-017-0049-x,
846 2018.

847 IPCC: Summary for Policymakers. In: IPCC Special Report on the Ocean and Cryosphere
848 in a Changing Climate [H.-O. Pörtner, D.C. Roberts, V. Masson-Delmotte, P. Zhai,
849 M. Tignor, E. Poloczanska, K. Mintenbeck, A. Alegría, M. Nicolai, A. Okem, J.
850 Petzold, B. Rama, N.M. Weyer (eds.)]. Cambridge University Press, Cambridge, UK
851 and New York, NY, USA, pp. 3–35. https://doi.org/10.1017/9781009157964.001,
852 2019.

853 Kargel, J. S., Leonard, G. J., Bishop, M. P., Kääb, A., and Raup, B. (Eds.): Global Land Ice
854 Measurements from Space (Springer-Praxis), 33 chapters, 876 pp.,
855 https://doi.org/10.1007/978-3-540-79818-7, 2014.

856 Kiernan, K., and McConnell, A.: Glacier retreat and melt-lake expansion at Stephenson
857 Glacier, Heard Island World Heritage Area. Polar Record. 38(207):297-308.
858 https://doi.org/10.1017/S0032247400017988, 2002.

859 Kirkbride, M. P, Dugmore, A. J.: Glaciological response to distaltephra fallout from the
860 1947 eruption of Hekla, south Iceland. Journalof Glaciology 49: 420–428.
861 https://doi.org/10.3189/172756503781830575, 2003.

862 Korneva, I. A., Toropov, P. A., Muraviev, A. Y., and Aleshina, M. A.: Climatic factors
863 affecting Kamchatka glacier recession. International Journal of Climatology, 1–25.
864 https://doi.org/10.1002/joc.8328, 2024.

865 Lambeth, A James.: "Heard Island. Geography and glaciology." Journal and proceedings
866 of the Royal Society of New South Wales 84(2), 92–98.
867 https://doi.org/10.5962/p.360589, 1951.

Lea, J. M., Mair, D. W. F., and Rea, B. R.: Evaluation of existing and new methods of tracking glacier terminus change. Journal of Glaciology. 60(220):323-332. https://doi.org/10.3189/2014JoG13J061, 2014.

Li, Z., England, M.H. and Groeskamp, S.: Recent acceleration in global ocean heat accumulation by mode and intermediate waters. Nat Commun 14, 6888. https://doi.org/10.1038/s41467-023-42468-z, 2023.

Mackintosh, A., Anderson, B., Lorrey, A., Renwick, J. A., Frei, P., and Dean, S. M.: Regional cooling caused recent New Zealand glacier advances in a period of global warming. Nat Commun 8, 14202. https://doi.org/10.1038/ncomms14202, 2017.

Maussion, F., Hock, R., Paul, F., Raup, B., Rastner, P., Zemp, M, Andreassen, L., Barr, I., Bolch, T., Kochtitzky, W., McNabb, R. and Tielidze, L: The Randolph Glacier Inventory version 7.0 User guide v1.0, doi:10.5281/zenodo.8362857. Online access: https://doi.org/10.5281/zenodo.8362857, 2023.

Mawson, D.: "The B.A.N.Z. Antarctic Research Expedition 1929-31." Geogr. Jour., 80, 105-6, 1932.

Millan, R., Mouginot, J., Rabatel, A. et al.: Ice velocity and thickness of the world's glaciers. Nat. Geosci. 15, 124–129. https://doi.org/10.1038/s41561-021-00885-z, 2022.

Mortensen, J., J. Bendtsen, R. J. Motyka, K. Lennert, M. Truffer, M. Fahnestock, and S. Rysgaard.: On the seasonal freshwater stratification in the proximity of fast-flowing tidewater outlet glaciers in a sub-Arctic sill fjord, J. Geophys. Res. Oceans, 118, 1382–1395, https://doi.org/10.1002/jgrc.20134, 2013.

Mölg, N., Bolch, T., Walter, A., and Vieli, A.: Unravelling the evolution of Zmuttgletscher and its debris cover since the end of the Little Ice Age, The Cryosphere, 13, 1889–1909, https://doi.org/10.5194/tc-13-1889-2019, 2019.

Nagai, H., Fujita, K., Sakai, A., Nuimura, T., and Tadono, T.: Comparison of multiple glacier inventories with a new inventory derived from high-resolution ALOS imagery in the Bhutan Himalaya, The Cryosphere, 10, 65–85, https://doi.org/10.5194/tc-10-65-2016, 2016.

Nel, W., Hedding, D. W., and Rudolph, E. M.: The sub-Antarctic islands are increasingly warming in the 21st century. Antarctic Science. 35(2):124-126. https://doi.org/10.1017/S0954102023000056, 2023.

Nield, J. M., Chiverrell, R. C., Darby, S. E., Leyland, J., Vircavs, L. H. and Jacobs, B.: Complex spatial feedbacks of tephra redistribution, ice melt and surface roughness modulate ablation on tephra covered glaciers. Earth Surf. Process. Landforms, 38: 95-102. https://doi.org/10.1002/esp.3352, 2013.

Oerlemans, J.: Glaciers and Climate Change, 160 Pages, ISBN 9789026518133. 2001.

Östrem, G.: Ice Melting under a Thin Layer of Moraine, and the Existence of Ice Cores in Moraine Ridges, Geogr. Ann., 41, 228–230, https://doi.org/10.1080/20014422.1959.11907953, 1959.

Paul, F., Svoboda, F.: A new glacier inventory on southern Baffin Island, Canada, from ASTER data: II. Data analysis, glacier change and applications. Annals of Glaciology. 50(53):22-31. https://doi:.org/10.3189/172756410790595921, 2009.

Paul, F., Barrand, N. E., Baumann, S. Berthier, E. Bolch, T. Casey, K. Frey, H. Joshi, S. P., Konovalov, V., Le Bris, R., Molg, N., Nosenko, G., Nuth, C., Pope, A., Racoviteanu, A., Rastner, P., Raup, B., Scharrer, K., Steffen, S., and Winsvold, S.: On the accuracy of glacier outlines derived from remote-sensing data, Ann. Glaciol., 54, 171–182, https://doi.org/10.3189/2013AoG63A296, 2013.

Perren, B. B., Hodgson, D. A., Roberts, S. J., Sime, L., Van Nieuwenhuyze, W., et al.: Southward migration of the Southern Hemisphere westerly winds corresponds with warming climate over centennial timescales. Communications Earth and Environment, 1, https://doi.org/10.1038/s43247-020-00059-6, 2020.

Pfeffer, W. T., Arendt, A. A., Bliss, A., Bolch, T., Cogley, J. G., Gardner, A. S., Hagen, J., Hock, R., Kaser, G., Kienholz, C., Miles, E. S., Moholdt, G., Mölg, N., Paul, F., Radic V., Rastner, P., Raup, B. H., Rich, J., Sharp, M. J., and The Randolph Consortium: The Randolph Glacier Inventory: a globally complete inventory of glaciers, J. Glaciol., 60, 537–552, https://doi.org/10.3189/2014JoG13J176, 2014.

Pockley, P.: Climate change transforms island ecosystem. Nature 410, 616. https://doi.org/10.1038/35070741, 2001.

Pohl, B., Saucède, T., Pergaud, J., Féral, J.-C., Richard, Y., Favier, V., et al.: Recent climate variability around the Kerguelen Islands (Southern Ocean) seen through weather regimes. Journal of Applied Meteorology and Climatology, 60, https://doi.org/10.1175/JAMC-D-20-0255.1, 2021.

Purdie, H., Anderson, B., Chinn, T., Owens, I., Mackintosh, A., Lawson, W.: Franz Josef and Fox Glaciers, New Zealand: historic length records. Glob. Planet. Change, 121, 41–52, https://doi.org/10.1016/j.gloplacha.2014.06.008, 2014.

Purdie, H., Bealing, P., Gomez, C., Anderson, B., and Marsh, O. J.: Morphological changes to the terminus of a maritime glacier during advance and retreat phases: Fox Glacier/Te Moeka o Tuawe, New Zealand. Geografiska Annaler: Series A, Physical Geography, 103(2), 167–185. https://doi.org/10.1080/04353676.2020.1840179, 2020.

Radić, V., Bliss, A., Beedlow, A.C. et al.: Regional and global projections of twenty-first century glacier mass changes in response to climate scenarios from global climate models. Clim Dyn 42, 37–58, https://doi.org/10.1007/s00382-013-1719-7, 2014.

Raup, B. H., Khalsa, S. J. S., Armstrong, R. L., Sneed, W. A., Hamilton, G. S., Paul, F., Cawkwell, F., Beedle, M. J., Menounos, B. P., Wheate, R. D., Rott, H., Shiyin, L., Xin, Li., Donghui, S., Guodong, C., Kargel, J. S., Larsen, C. F., Molnia, B. F., Kincaid, J. L., Klein, A., and Konovalov, V.: Quality in the GLIMS glacier database, in: Global Land Ice Measurements from Space, edited by: Kargel, J. S., Leonard, G. J., Bishop, M. P., Kääb, A., and Raup, B. H., Springer Berlin Heidelberg, 163–182, https://doi.org/10.1007/978-3-540-79818-7_7, 2014.

Richardson, J. M., and Brook, M. S.: Ablation of debris-covered ice: someeffects of the 25 September 2007 Mt Ruapehu eruption. Journal of theRoyal Society of New Zealand 40: 45–55. https://doi.org/10.1080/03036758.2010.494714, 2010.

Rivera, A., Bown, F., Carrion, D., and Zenteno, P.: Glacier responses torecent volcanic activity in southern Chile. Environmental Research Letters 7: 014036. https://doi.org/10.1088/1748-9326/7/1/014036, 2012.

Rounce, D. R., Hock, R., Maussion, F., Hugonnet, R., Kochtitzky, W., Huss, M., Berthier, E., Brinkerhoff, D., Compagno, L., Copland, L. and Farinotti, D.: Global glacier change in the 21st century: Every increase in temperature matters. Science, 379(6627), pp.78-83. https://doi.org/10.1126/science.abo1324, 2023.

Scherler, D., Bookhagen, B., and Strecker, M. R.: Spatially variable response of Himalayan glaciers to climate change affected by debris cover, Nat. Geosci., 4, 156–159, https://doi.org/10.1038/NGEO1068, 2011.

Soci, C., Hersbach, H., Simmons, A., Poli, P., Bell, B., Berrisford, P., et al.: The ERA5 global reanalysis from 1940 to 2022. Quarterly Journal of the Royal Meteorological Society, 150(764), 4014–4048. Available from: https://doi.org/10.1002/qj.4803, 2024.

Straneo, F., and C. Cenedese.: The dynamics of Greenland's glacial fjords and their role in climate, Ann. Rev. Mar. Sci., 7, 89–112, https://doi.org/10.1146/annurev-marine-010213-135133, 2015.

Stokes, C. R., Shahgedanova, M., Evans, I., and Popovnin, V. V.: Accelerated loss of alpine glaciers in the Kodar Mountains, south-eastern Siberia, Glob. Planet. Change, 101, 82–96, https://doi.org/10.1016/j.gloplacha.2012.12.010, 2013.

Truffer, M., and R. J. Motyka.: Where glaciers meet water: Subaqueous melt and its relevance to glaciers in various settings, Rev. Geophys., 54, 220––239 https://doi.org/10.1002/2015RG000494, 2016.

Tachikawa, T., Hato, M., Kaku, M., and Iwasaki, A: Characteristics of ASTER GDEM version 2. In 2011 IEEE international geoscience and remote sensing symposium (pp. 3657-3660). IEEE. https://doi.org/10.1109/IGARSS.2011.6050017, 2011.

Thost, D. E., and Truffer, M.: Glacier Recession on Heard Island, Southern Indian Ocean. Arctic, Antarctic, and Alpine Research, 40(1), 199–214. https://doi.org/10.1657/1523-0430(06-084)[THOST]2.0.CO;2, 2008.

Tielidze, L. G.: Glacier change over the last century, Caucasus Mountains, Georgia, observed from old topographical maps, Landsat and ASTER satellite imagery, The Cryosphere, 10, 713–725, https://doi.org/10.5194/tc-10-713-2016, 2016.

Tielidze, L. G. and Wheate, R. D.: The Greater Caucasus Glacier Inventory (Russia, Georgia and Azerbaijan), The Cryosphere, 12, 81–94, https://doi.org/10.5194/tc-12-81-2018, 2018.

Tielidze, L. G., Bolch, T., Wheate, R. D., Kutuzov, S. S., Lavrentiev, I. I., and Zemp, M.: Supra-glacial debris cover changes in the Greater Caucasus from 1986 to 2014, The Cryosphere, 14, 585–598, https://doi.org/10.5194/tc-14-585-2020, 2020.

Tielidze, L. G., Nosenko, G. A., Khromova, T. E., and Paul, F.: Strong acceleration of glacier area loss in the Greater Caucasus between 2000 and 2020, The Cryosphere, 16, 489–504, https://doi.org/10.5194/tc-16-489-2022, 2022.

Vieli, A.: Tidewater Glaciers. In: Singh, V.P., Singh, P., Haritashya, U.K. (eds) Encyclopedia of Snow, Ice and Glaciers. Encyclopedia of Earth Sciences Series. Springer, Dordrecht. https://doi.org/10.1007/978-90-481-2642-2_579, 2011.

Weber, P., Andreassen, L. M., Boston, C. M., Lovell, H., and Kvarteig, S.: An ~1899 glacier inventory for Nordland, northern Norway, produced from historical maps. Journal of Glaciology 1–19. https://doi.org/10.1017/jog.2020.3, 2020.

Williamson, R. A.: The Landsat legacy: Remote sensing policy and the development of commercial remote sensing. Photogrammetric Engineering and Remote Sensing, 63, 877-885. 1997.

Zemp, M., M. Huss, E. Thibert, N. Eckert, R. McNabb, J. Huber, M. Barandun, H. Machguth, S. U. Nussbaumer, I. Gartner-Roer, et al.: Global glacier mass changes and their contributions to sea-level rise from 1961 to 2016. Nature 568 (7752):382–86. https://doi.org/10.1038/s41586-019-1071-0, 2019.